UNIVERSITY OF OKLAHOMA

GRADUATE COLLEGE

AN ANALYTICAL MODEL TO DETERMINE A RESERVOIR CAPACITY FOR WASTEWATER DISPOSAL WITH CONSIDERATION OF GEOMECHANICS AND EXTRACTIONS

A THESIS

SUBMITTED TO THE GRADUATE FACULTY
in partial fulfilment of the requirements for the

Degree of

MASTER OF SCIENCE

By

FNU SRIJAN
Norman, Oklahoma
2025

Downloaded from SHAREOK. Persistent Handle URL: https://hdl.handle.net/11244/341360

AN ANALYTICAL MODEL TO DETERMINE A RESERVOIR CAPACITY FOR WASTEWATER DISPOSAL WITH CONSIDERATION OF GEOMECHANICS AND EXTRACTIONS

A THESIS APPROVED FOR THE
MEWBOURNE SCHOOL OF PETROLEUM AND GEOLOGICAL ENGINEERING

BY THE COMMITTEE CONSISTING OF

Dr. Xingru Wu, Chair

Dr. Mashhad Fahes

Dr. Bor-Jier (Ben) Shiau

© Copyright by FNU SRIJAN 2025
All Rights Reserved.

Acknowledgments

I have been working on this research for two years and it is impossible to complete the task on my own. Many people provided their support, guidance and encouragement to me.

First and foremost, I would like to express my heartfelt gratitude to my advisor, Dr. Xingru Wu, for his unwavering support and patience throughout this project. His guidance and encouragement have been invaluable to me academically and personally. I have learned so much from his example about what it means to be a thoughtful engineer and an inspiring mentor. This thesis would not have been possible without his steady supervision and belief in my abilities.

I am also deeply thankful to Dr. Mashhad Fahes and Dr. Ben Shiau for their time, expertise, and thoughtful feedback as members of my committee. Their insights have pushed me to think critically and improve my work.

Lastly, I want to thank my parents for their constant love and encouragement during my years of study and throughout this journey. Their belief in me has always been my greatest strength. Thank you to all my friends for being my rock and offering me endless support and motivation.

This achievement is as much theirs as it is mine.

Srijan

Contents

ABSTRACT vii
1. Introduction 1
1.1. Objectives and Motivation 1
1.2. Key Issues and Challenges 2
1.3. Contribution of this Research 4
1.4. Thesis Organization 5
2. Literature Review 8
2.1. Introduction 8
2.2. Fundamentals of Geomechanical Constraints and the Factors Influencing Them 9
2.2.1. In-situ stress 10
2.2.2. Vertical Stress 11
2.2.3. Horizontal Stress 12
2.2.4. Tectonic stress 14
2.2.5. Poroelastic stress 15
2.2.6. Thermoelastic stress 16
2.2.7. Water Quality 17
2.3. Importance of fracture gradient and the methods to predict it 18
2.3.1. Understanding the mud losses while drilling 19
2.3.2. Methods to predict the fracture gradient 20
- *Hubbert–Willis. Hubbert and Willis* 20
- *Matthews and Kelly Method* 21
- *Ben Eaton Method* 21
2.4. Analytical vs. Numerical Approaches in Injection Volume Estimation 22
2.5. Pressure Superposition and its Effects on Injection Efficiency 23
2.6. Uncertainty Analysis incorporated in this model 25
2.7. Summary of Research Opportunities 28
3. Methodology 29
3.1. Analytical solution to predict the pressure in a reservoir with multiple production/injection wells 29
3.2. Applied geomechanical model in this research 30
3.3. Determining the Maximum Injection Capacity for a Reservoir 32
3.4. Case Study to Predict Pressure Distribution and Maximum Injection Capacity 33
3.5. Determination of well injectivity before and after the fracture formation 39
3.6. Relationship between Injection Pressure and Injection Rate 41
3.6.1. Determination of friction in the injected string (P_friction) 42

3.6.2. Bottomhole pressure and hydrostatic head pressure.....44
3.6.3. Determination of surface pressure.....45
3.7. Validation of Analytical model through numerical model results 46
4. Results and Conclusions.....50
References.....54

Table of Figures

Figure 1- Comparison of cost for disposal methods (Sahu 2021), and the darkening bar indicates the range of costs 3
Figure 2- Numerical model of 16 equally spaced water injection wells.....5
Figure 3-Plan view of vertical fracture perpendicular to the horizontal earth stress. Adapted from Perkins & Gonzalez (1985)..... 22
Figure 4-Fracturing and determination of the breakdown pressure from a leak off test. Adapted from (Wu 2017).....25
Figure 5-The concept of project and reservoir areas with mutilple wells.....35
Figure 6-Wells in the project region. The project area is around 150,000 acres with 274 wells.....34
Figure 7- Histograms showing the frequencies of reservoir properties. True vertical depth and net-pay thickness are from well database, and porosity, pore volume compressibility are calculated from correlations.....36
Figure 8-Pressure heat map in the project area calculated by pressure superposition of all wells. The blue multi-segment line is a hypothetical pressure sensitive region for reservoir surveillance. 37
Figure 9-Distribution of fracturing pressure for the formation interval in the project area using MC simulation with LHS algorithms. P10 means the probability of fracturing pressure less than 7362 psi is less than 10%. 38
Figure 10-Distribution of additional injection volume before the rock fails in the project area. 39
Figure 11-Pressure display after 15 years of water injection estimated by numerical modeling 48
Figure 12- Graphical representation of pressure spikes near the injection point.....48
Figure 13- Graphical representation of liquid rate in standard conditions vs the time in days49

ABSTRACT

In many scenarios, we need to determine the capacity of a reservoir for water injection or disposal. The capacity is typically controlled by the container size, total compressibility, and the maximum pressure above which the injection may jeopardize the formation integrity related to formation parting pressure. It can be potentially correlated to and sometimes even cause fault reactivation. Even though current studies only have correlations rather than causality to prove that SWD causes fault reactivation, it has been established that other factors like permeability, reservoir fluid, and mineralogy can also be potential factors causing seismic activities. Given that full-scale numerical modeling and simulation needs extensive data that isn't usually available, we propose an analytical model to determine the maximum injection volume based on pressure superposition. This model provides a practical solution to calculate the reservoir capacity that can help fill knowledge gaps by removing human bias.

In the proposed model, a reservoir container has homogeneous properties with boundaries that can be infinite acting, open, or closed. Multiple wells, including injection (disposal) wells and extraction wells, are arbitrarily placed in the reservoir. The model assumes that individual extraction rates are constant with time but may differ from well to well. A geomechanical model considering thermoelastic and poroelastic stresses determines the maximum injection pressure. An equation system can be established for injection wells to a given time based on the pressure superposition in the reservoir. The solution of the equation system is the rates for the injection wells.

The analytical solution is validated by numerical simulation with 16 equally spaced wells in a 100 km by 100 km reservoir with closed boundaries, and the reservoir only contains water. We get the amount of water volume and pressure profiles at different times through numerical modelling. We use the determined rates from the equation system and known extraction rates

to compute the pressure along the fault to see when the activation pressure is reached. With known rates and time, the reservoir's total capacity can be determined.

The proposed analytical model is robust, easy to implement, and doesn’t need extensive subsurface characterization. Because of its high performance, the model can be used in uncertainty studies, such as Monte Carlo simulation, to determine the range of capacity with probability. This will make the model very attractive in practice. This geomechanical approach is a valuable tool that can provide optimal water injection pressure while minimizing the risk of formation integrity.

1. Introduction

1.1.Objectives and Motivation

Nowadays water injections are one of the most widely adopted technologies for maintaining reservoir pressure and enhancing oil recovery. Hassan et al. (2023) also stated that the water injection method is the most well-established secondary oil recovery technique. Each of these EOR approaches has its own set of challenges and preferences when it comes to the environment where it is used. We all know that during the water injection operation, the injection volume of the reservoir increases, and the reservoir becomes more complex, so determining the exact capacity of the reservoir is a major task. If injection pressure exceeds the fracture pressure, it can lead to fracturing, fault reactivation, and sometimes even cause induced seismicity. Therefore, it leads to an important research topic of determining the capacity of the water injection in a well to maintain the reservoir integrity.

Many researchers have explored the traditional approaches for estimating the reservoir capacity, using empirical models and numerical simulations, to determine maximum injection volume. This thesis focuses on developing an analytical model that does not require extensive sub-surface data making it more practical as it is not always attainable. This model offers a faster and more efficient way to estimate reservoir capacity, that also accounts for pressure superposition, geomechanical constraints, and uncertainty in subsurface properties without being computationally expensive.

The primary objective of this research is to develop a robust analytical model that can accurately determine the maximum allowable water injection volume while incorporating geomechanical constraints and pressure superposition effects. To achieve this goal, four major tasks are undertaken in this thesis:

1. Developing a new analytical model that estimates the injection volume by considering pressure interactions between wells and geomechanical constraints.
2. Extending the model to be applicable for both single-well and multi-well reservoir systems, ensuring its usability across various reservoir conditions.
3. Validating the model through numerical simulations and benchmarking against field data, ensuring its reliability for practical applications in reservoir engineering.

By addressing these challenges, this research aims to provide a computationally efficient, easy-to-implement, solution for optimizing water injection operations while maintaining reservoir integrity and preventing environmental risks.

1.2.Key Issues and Challenges

The development and production of oil and gas generate substantial volumes of wastewater, primarily in the form of produced water. Much of this wastewater is managed through underground injection into saltwater disposal (SWD) wells. In 2017 alone, approximately 24.4 billion barrels of produced water was generated by nearly one million oil and gas wells across the United States. While there is growing interest in the beneficial reuse of produced water (Scanlon et al. 2020), a significant portion continues to be disposed of via injection. Additionally managing the produced water is a major concern in the oil and gas industry. The proportion of produced water that is recycled versus disposal varies by region and over time; however, disposal remains the dominant management practice nationwide. According to the U.S. Geological Survey, over 95% of produced water from hydrocarbon extraction is injected underground, either into dedicated disposal wells regulated under the Underground Injection Control (UIC) program or into petroleum reservoirs for enhanced oil recovery (EOR) and pressure maintenance (Clark and Veil 2009). The decision of disposal method is a balance of cost and disposal regulations in a particular area, and Figure 1 shows the costs for different water treatment methods.

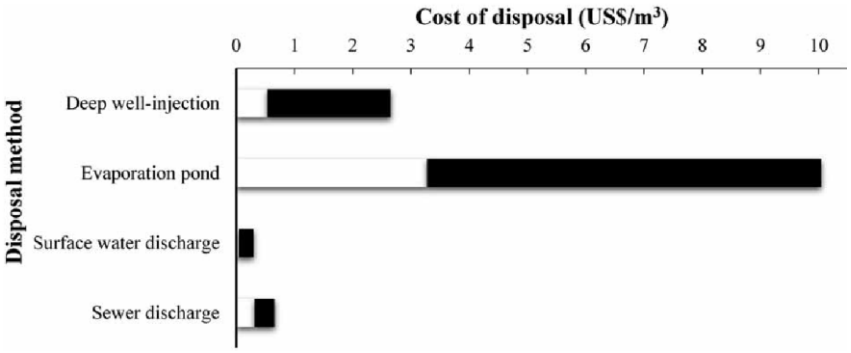


Figure 1- Comparison of cost for disposal methods (Sahu 2021), and the darkening bar indicates the range of costs

Field experience underscores the importance of designing disposal wells with a comprehensive understanding of key operational parameters, including maximum injection rates and pressures, formation breakdown pressures, and the overall storage capacity of the disposal zone. Proper engineering and monitoring of disposal wells are critical to mitigating environmental risks and preventing unintended consequences such as induced seismicity, formation damage, or fluid migration.

Determination of the maximum allowable injection pressure in SWD or water injection operations is very crucial, exceeding this threshold can lead to unintended fracture propagation which may cause formation integrity failure. The maximum injection capacity is controlled by the pore volume and pressure dissipation capability of the reservoir. Without proper pressure monitoring, disposal wells may reach injectivity limits prematurely.

To address these challenges, we propose an analytical model that uses pressure superposition to determine the maximum injection volume for a reservoir in this paper. The model aims to provide a practical solution that can estimate the reservoir capacity without extensive data gathering or complex simulations. By considering a homogeneous reservoir with various boundary conditions like infinite, closed, and open boundaries and multiple wells (both injection and extraction), this model simplifies the process of reservoir capacity estimation while ensuring that the maximum injection pressure remains within safe limits, thus preserving formation integrity. In this study, Monte Carlo simulation was employed to account for possible

parameter distributions, providing a range of potential pressures and their associated probabilities of occurrence.

1.3.Contribution of this Research

The contributions of this research lie in the development of an analytical model that accurately determines the maximum injection volume for water injection and disposal wells while considering geomechanical constraints and pressure superposition effects.

In this study, we present the pressure superposition model. Then, this model will be applied to a selected region that contains multiple formation intervals and numerous injection and water disposal/injection wells. The pressure superposition yields the pressure (or pressure differential) heat map, which can help place target injection wells. We apply a geomechanics model to determine the fracturing pressure, which is used as the maximum injection pressure and the maximum pressure the interval can have. The maximum injection volume (reservoir remaining capability) is determined by applying determined reservoir properties. Finally, this model uses pressure superposition to estimate the pressure distribution along a multi-segment line regarded as a sensitive region.

This study employs a numerical model, focusing on pressure behavior in a 10 km × 10 km reservoir during water injection operations. The reservoir was modeled with sixteen equally spaced water injection wells, strategically positioned as illustrated in Figure 2. Comprehensive input parameters, including rock and fluid properties, are detailed in Table 2 to ensure an accurate representation of reservoir conditions.

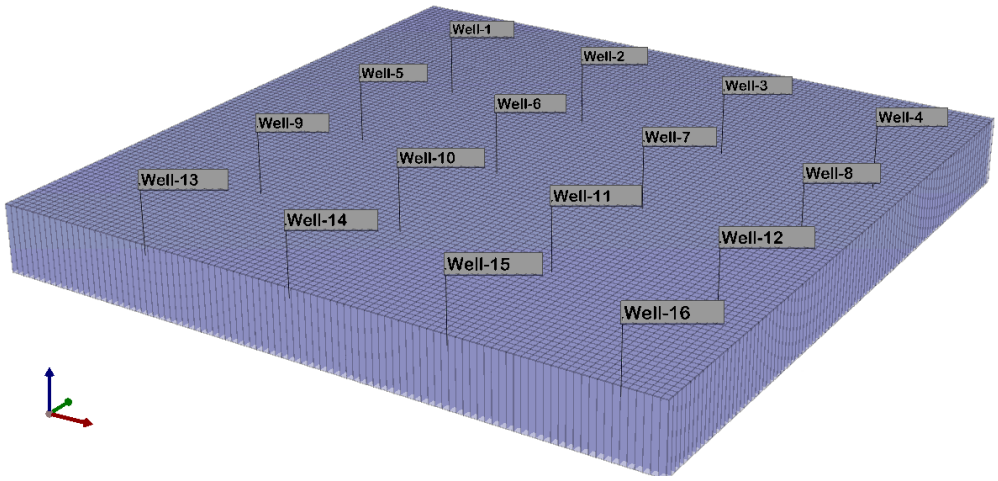


Figure 2- Numerical model of 16 equally spaced water injection wells

The numerical simulation was developed using an industry-standard reservoir simulator to evaluate bottomhole pressure (BHP) dynamics under continuous water injection. The simulation was initialized with a BHP of 8,000 psi and a water injection rate of 3,000 barrels per day (bbl/day). The model was run for 15 years, during which the maximum recorded BHP was carefully monitored to ensure it remained within safe operational limits, preventing fault reactivation or fracture initiation. Given the significant uncertainty in subsurface parameters and the lack of precise, accurate values, we typically only have a general range of these parameters. To address this, we incorporated stochastic modeling, alongside analytical and numerical approaches, to determine the maximum allowable pressure for water injection wells.

1.4.Thesis Organization

This thesis is mainly divided into 5 major chapters:

- Chapter 1: Introduction

  This chapter talks about the importance of water injection and SWD in reservoir management as it produces large amounts of wastewater. Improper balancing of

wastewater disposal can lead to serious consequences such as fault reactivation, and formation fracturing or could even trigger seismic activities. Therefore, it becomes very crucial to determine the injection capacity of a reservoir while staying within the safe geomechanical limits. To address this challenge, we have developed an analytical model based on the pressure superposition principles. This model considers multiple injection and extraction wells within various boundary conditions and incorporates poroelastic and thermoelastic geomechanical constraints to estimate the maximum injection volume. Ultimately, this chapter establishes the motivation, challenges, and objectives of the research.

- Chapter 2: Literature Review

  This chapter presents a comprehensive review of existing research and industry practices in reservoir geomechanics, water injection, and saltwater disposal. It begins with outlining the geomechanical factors that influence injection operations such as the stresses, pore pressure, rock strength, etc. This chapter also examines various methods to predict the fracture gradient including the direct methods like LOT and the already existing empirical models like Hubbert-Willis or Ben Eaton methods. Then it emphasizes the importance of considering the pressure superposition principle for modeling in muti-well interactions.

  Finally, it highlights the importance of incorporating uncertainty analysis in the model through Monte Carlo simulation.

- Chapter 3: Methodology

  This chapter details the development of the analytical model for estimating the reservoir capacity, integrating both the geomechanical constraints and the pressure superposition effects. The importance of these constraints was explained in Chapter 2. Then chapter

3 begins by the concept of the multi-well reservoir system and outlines the assumptions that we have made for this model.

Next, comes the two geomechanical models that are applied in this research to determine the maximum injection pressure for a reservoir.

Then this chapter describes how reservoir characterization was performed using the historical well data obtained from Enverus to estimate parameters like porosity, net thickness, and compressibility. Pressure superposition is applied to estimate the reservoir pressure distribution over time. Finally, this chapter highlights the relationship between injection pressure and injection rate with the determination of injectivity index before and after the fracturing of the well.

- Chapter 4: Results and Conclusions

  This chapter summarizes the key findings of the research and outlines the broader implications of the proposed analytical model for saltwater disposal (SWD) well design and reservoir capacity estimation. The study demonstrates that integrating geomechanical considerations—such as in-situ stress, poroelastic and thermoelastic effects—into an analytical pressure superposition framework can provide a reliable estimate of the maximum injection volume for a reservoir. The model's accuracy is validated through numerical simulations and enhanced through uncertainty quantification using Monte Carlo simulation with Latin Hypercube Sampling.

  The conclusions emphasize that maintaining injection pressures below the fracture gradient is critical for preserving reservoir integrity and minimizing seismic risk. The methodology presented offers a scalable, computationally efficient alternative to full numerical models, making it suitable for early-stage field assessments, regulatory evaluations, and operational planning.

2. Literature Review

2.1.Introduction

The design of a SWD well requires careful evaluation of key operational parameters such as maximum injection pressure, injection capacity, and formation integrity to ensure long-term operational efficiency and environmental safety. Among them, one of the most critical design parameters is the maximum allowable injection pressure, which is dictated by the fracturing pressure gradient of the target formation (Murray 2014). Exceeding this threshold can cause unintended fracture propagation, leading to the loss of containment, migration of injected fluids, and potential communication with shallower groundwater-bearing zones. To prevent such cases, regulatory agencies in the United States, such as state-level commissions, have imposed strict pressure limits to prevent formation damage and contamination risks (Schmidt et al. 2021). Therefore, accurate estimation of the fracture gradient, combined with real-time monitoring of wellhead and bottom hole pressures, is essential to maintain injection integrity and prevent geomechanical failure (Khan and Michael 2024).

Another fundamental consideration of the SWD design is the maximum injection capacity of the disposal formation, which is controlled by its pore volume, and pressure dissipation capability (Clement Okezie and Bump 2024). The injectivity index of an SWD determines the sustainable disposal rate before pressure buildup becomes excessive. If the formation has limited permeability, prolonged injection can lead to pore pressure elevation near the wellbore, reducing the effectiveness of disposal operations. Additionally, prolonged high-pressure injections may activate pre-existing faults, potentially triggering induced seismicity. Disposal wells should also be designed with multiple monitoring points, and downhole pressure gauges may be used to track pressure evolution over time and detect early signs of reservoir over-pressurization.

A saltwater disposal well's overall design and management must incorporate comprehensive injection surveillance protocols to ensure compliance with regulatory requirements and operational safety. Operators can optimize disposal performance by integrating advanced geomechanical modeling, real-time pressure monitoring, and regulatory-compliant operational limits while minimizing subsurface hazards.

The correlations currently established between the saltwater disposal and the seismic activities potentially triggered by these injection practices do not have any direct causality; it is widely accepted that factors like permeability, reservoir fluid properties, and mineralogy also contribute to the risk of fault reactivation. Additionally, understanding reservoir geomechanical behavior is increasingly vital for the petroleum industry as it plays a crucial role in safe and efficient reservoir management.

Hamid et al. (2017) observed that substantial changes in pore pressure, whether from depletion or injection activities, can lead to significant shifts in effective stress, particularly in weak formations. These changes in stress can impact the stability of the reservoir rock, leading to potential issues such as wellbore instability, fault re-activation, and unwanted fracture propagation.

In the next section, the existing research that informs the development of the proposed model will be reviewed. The crucial factors and their significance that have been incorporated into the model for injection safety will also be highlighted.

2.2.Fundamentals of Geomechanical Constraints and the Factors Influencing Them

The pressure required to fracture a rock formation is closely tied to the stresses within the Earth's crust and the mechanical properties of the rock (Morgenstern 1962).This relationship suggests that understanding rock strength and estimating local stress conditions makes it possible to predict the pressures needed to induce fractures.

A geomechanical model needs to be built to predict stress-induced wellbore failure. The principal constituents of the geomechanical model are the three principal stresses: vertical stress (σ_v), Maximum principal horizontal stress (σ_H), minimum principal horizontal stress (σ_h), pore pressure (p_p), and the rock strength parameter Unconfined Compressive Strength (UCS). Three types of stress field distribution have been noted with $\sigma_H > \sigma_h > \sigma_v$ found mainly in relatively shallow coal mines (<400 m), the $\sigma_H > \sigma_v > \sigma_h$ type in moderately deep coal mines (400–600 m), and the $\sigma_v > \sigma_H > \sigma_h$ type predominantly in moderately deep to deep coal mines (Kang 2010) .When the horizontal stresses are not equal (a frequent condition in the Earth's crust), stress anisotropy is created. Pore pressure is a critical parameter in the geomechanical model and can be directly related to fracture gradient, especially in depleted formations. Rock strength is also a major input in the calculation of wellbore collapse. When these parameters are known, a geomechanical model can be created and utilized for various applications, including evaluation of wellbore stability, injection pressure constraints, and sand/solids production prediction(Aamri et al. 2017).

2.2.1. In-situ stress

In-situ stress is the stress of a subsurface formation. Variation of the in-situ stress state is closely related to engineering geological hazards, sliding instability of crustal fracture, and earthquake preparation. The study of in situ stress measurement and its distribution characteristics has always been a basic and very important task in rock mechanics and geodynamics. The measured in situ stress data can not only directly reflect the characteristics of the regional in situ stress field and the distribution characteristics of the in situ stress in the engineering area but also can determine the properties of engineering rock mass for stability analysis of surrounding rock and support structure design (Li et al. 2017). It is commonly characterized by three principal perpendicular stresses: overburden stress, maximum horizontal stress, and

minimum horizontal stress. In other orientations, stress components devolve into a tensor characterized by directionality and magnitude, and they include normal stress and shear stress components relative to the surface upon which the stress is acting (Ma 2016). Accurately understanding stress ranges is essential for effective geomechanical modeling. Errors in estimating horizontal stress can result in inefficient wellbore designs and higher operational expenses. For instance, miscalculating in-situ stresses in overpressure environments can greatly affect porosity-permeability measurements during core analysis and compromise pore volume compressibility data used in reservoir simulations.

2.2.2. Vertical Stress

The concept of in situ stress was first put forward by Swiss geologist Albert Heim, who believed that the magnitude of the vertical stress was related to the buried depth and vertical stress was equal to horizontal stress in the absence of tectonic influences (K=1, K is discussed in Eqn 2.6) (Arno 2010). This foundational idea laid the groundwork for understanding stress distributions in the Earth's crust, particularly in geomechanics and structural geology. Heim's work emphasized the role of depth in determining stress magnitudes, forming the basis for modern stress analysis in subsurface formations.

M.R.P. Tingaya (2002) highlighted that vertical or lithostatic stress is critical in tectonic and geomechanical studies, particularly for predicting pore pressures and fracture gradients. However, it is often not measured in situ, and a standard approximation of 1.0 psi/ft (22.63 MPa/km) is commonly applied for the vertical stress gradient.

The vertical stress, also known as the overburden stress, can be calculated at the given depth D, as

$$\sigma_v = g \int_0^D \varrho \, \mathrm{d}D \tag{2.1}$$

Where,

σ_v -vertical or overburden stress (Pa)

ρ -formation bulk density (kg/m^3)

g -gravitational acceleration (m/s^2)

D -depth (m)

In the case of porous medium, the weight of the overburden is carried by both the rock material and the fluid within the pore space. The corresponding effective vertical stress can be calculated by:

$$\sigma'_v = \sigma_v - \alpha p \tag{2.2}$$

Where,

α -biot's poroelastic constant

p - pore pressure.

Hydrostatic pore pressure is defined as the weight of a vertical column of water from the sea surface to the depth of interest(Aamri et al. 2017).The Biot coefficient (α) quantifies the relationship between pore pressure and effective stress in porous materials, with values typically ranging from 0 to 1. A Biot coefficient of 0.7 indicates that 70% of the applied stress is transmitted through the pore fluid, while the solid matrix bears the remaining 30% (Salemi et al. 2021).

2.2.3. Horizontal Stress

The magnitude of the least principal stress (σ_h) can be determined from an active measurement (such as mini frac, leak-off tests, extended leak-off tests, wireline fracking, etc.), indirectly

from log-based methods (e.g., Eaton) or core-based methods (inelastic strain recovery, differential stress analysis, or Kaiser effects). Direct testing is more reliable than an indirect derivation from logs.(Aamri et al. 2017).Case study shows that the naturally fractured formation with high dip-angle or vertical fractures has a lower minimum horizontal stress (Zhang et al. 2023).

The effective horizontal stress σ'_H can be translated from vertical stress through the Poisson relationship:

$$\sigma'_H = \frac{\nu}{1-\nu}\sigma'_v \tag{2.3}$$

Where,

υ -Poisson's ratio

For most materials, Poisson's ratio typically falls between 0.2 and 0.5, with metals commonly having a value around 0.3. However, there are exceptions. For instance, a cork (cork refers to the material commonly used for bottle stoppers) has a Poisson's ratio close to 0, meaning it hardly changes shape in directions perpendicular to an applied stress. Some materials known as auxetic materials have negative Poisson's ratios, which causes them to expand in all directions when subjected to tensile strength.

The absolute horizontal stress, S_H, can be determined as follows:

$$\sigma_H = \sigma'_H + \alpha p \tag{2.4}$$

As a result of tectonic stresses, the horizontal stress is not the same in all directions in the horizontal plane. Therefore, there is minimum horizontal stress and maximum horizontal stress, which can be defined as:

$$\sigma_{H,max} = \sigma'_{H,min} + \sigma_{tect} \quad (2.5)$$

Where,

σ_{tect} refers to the tectonic stress

2.2.4. Tectonic stress

Ali et al. (2022) concluded that tectonic characteristics create conditions conducive to seismic activity, often leading to earthquakes along associated fault lines. Gaining a thorough understanding of these tectonic settings is crucial for evaluating stress regimes, seismic risks, and the overall geological behavior of the region.

Tectonic processes influence the in-situ stresses and can even change the arrangements in tectonically active regions. According to Zoback (2002), the stress in the brittle upper crust is dominated by large-scale tectonic processes. Based on Anderson's faulting theory Anderson (1951), the arrangement of principal stresses can be related to the style of currently active faults induced by a given tectonic regime in a region. According to Anderson's faulting theory, in normal faulting (N) regime σ_V is the greatest principal stress and σ_h is the least principal stress at depth ($\sigma_V > \sigma_H > \sigma_h$), and therefore, the value of K in this regime is<1, while in the reverse faulting (RF) regime the stress field is very compressive. Both horizontal stresses exceed the vertical stress ($\sigma_H > \sigma_h > \sigma_V$) and, therefore, the value of K in this regime is always >1. The strike-slip faulting (SS) regime represents an intermediate stress state where the vertical stress is greater than the minimum horizontal stress and less than the maximum horizontal stress ($\sigma_H > \sigma_V > \sigma_h$), thus the value of K in this regime is about 1, where K can be defined as:

$$K = 0.5\frac{\left(\sigma_h + \sigma_H\right)}{\sigma_v} \quad (2.6)$$

2.2.5. Poroelastic stress

Poroelasticity describes the physical process of rock deformation and fluid flow through deformable pores, more accurately estimating the changes in stress and pore pressure within the crust. Chang and Segall (2016) most models neglect poroelastic stress changes associated with injection, assuming that direct pore pressure changes are the dominant effect in destabilizing faults. However, indirect stress transfer may perturb faults without direct diffusion of pore pressure. Due to poroelastic coupling, fluid injection or extraction can induce seismicity by changing stress fields in rocks adjacent to the storage formation (Segall and Lu 2015).

The change in the pore pressure due to the injection can induce the poroelastic stress in the formation rock, the poroelastic stress at the wellbore wall Biot and Willis (2021) can be defined as –

$$\Delta\sigma^{P} = \alpha_{P}\Delta P \tag{2.7}$$

With the effect of the geometry of the thermal front,

$$\Delta\sigma^{P} = S_{f}\frac{\alpha_{p}E\Delta P}{1-\nu} \tag{2.8}$$

α_p the coefficient of the pore pressure defined as,

$$\alpha_{p} = \alpha\frac{1-2\nu}{1-\nu} \tag{2.9}$$

Where,

α is Biot's poroelastic constant

2.2.6. Thermoelastic stress

Thermoelastic stress refers to the changes in stress within a rock formation caused by variations in temperature. Lu et al. (2019) provided a modified method to accurately predict fracture initiation pressure, considering thermal and plugging effects. The paper concluded that temperature variations around the perforated wellbore induce thermal stress during cold or hot water injection. The thermal stress induced by cold water injection reduces the fracture initiation pressure (FIP) of water injection wells, whereas hot water injection has the opposite effect. Furthermore, the formation rock is more likely to fracture during cold water injection.

When a cool fluid such as water is injected into a hot reservoir, a growing region of cooled rock is established around the injection well. The rock matrix within the cooled region contracts and a thermoelastic stress field is induced around the well. This is referred to as injection thermoelastic stress(Perkins and Gonzalez 1985).

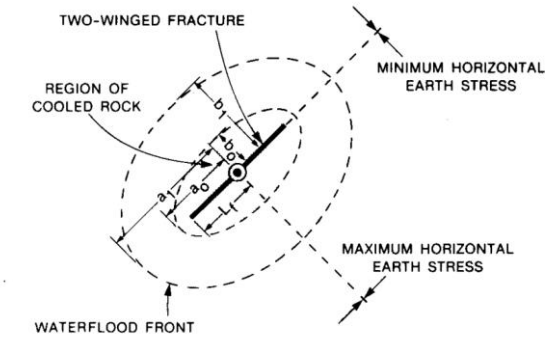


Figure 3 -Plan view of vertical fracture perpendicular to the horizontal earth stress. Adapted from Perkins & Gonzalez (1985)

Perkins and Gonzalez (1985) developed a numerical method to calculate the change in horizontal earth stress resulting from a step change in temperature (or pressure) across a region of elliptical cross-section and finite thickness.

$$S_f = \frac{\Delta\sigma^T(1-\nu)}{\alpha_T E \Delta T} \tag{2.10}$$

Where,

Δ T: temperature difference between the injected fluid and formation temperature

S_f: geometric shape factor of the cooled region of the reservoir rock.

α_T is the coefficient of thermoelastic stress

According to (Perkins and Gonzalez 1985) , S_f can be measured as

$$S_f = \frac{\left(\frac{b_o}{a_o}\right)}{1+\left(\frac{b_o}{a_o}\right)} \tag{2.11}$$

Where ao is the major semi-axis, and bo is the minor semi-axis of the elliptical cooling region, as shown in Figure 4.

The degree of thermoelastic stress depends on several factors, including the thermal expansion coefficient of the rock, the temperature difference between the fluid and the formation, and the rock's elastic properties such as Young's modulus and Poisson's ratio. In some cases, heating the formation may lead to compressive stresses, potentially closing fractures instead of extending them. The interaction between thermoelastic stress and the in-situ stresses in the reservoir plays a crucial role in determining how fractures propagate.

2.2.7. Water Quality

Poor injection water quality is a prime factor in reducing injectivity in many water injections and disposal wells. These reductions in injectivity often result in costly workovers, stimulation jobs, and re-completions, or, in many cases, the uncontrolled fracturing of wells by high bottom hole pressures, resulting in poor water injection conformance and reduced overall sweep efficiency and recovery (Bennion et al. 1998).

Thus, ensuring that water quality does not adversely impact injectivity is crucial. Poor water quality can lead to severe operational challenges, such as restricted water injection, voidage replacement inefficiencies, and uncontrolled fracture propagation, which can compromise the overall efficiency of waterflooding and disposal operations. Maintaining optimal water quality through effective treatment and monitoring is essential to prevent interactions that may degrade injectivity, ensuring sustained reservoir performance and operational success(Bennion et al. 1998).

2.3. Importance of fracture gradient and the methods to predict it

The design and operation of SWD wells require a thorough assessment of the maximum allowable injection pressure to ensure safe and efficient disposal while minimizing risks such as induced seismicity and reservoir damage. A key parameter in this assessment is the fracturing pressure gradient, which dictates the upper limit of injection pressure to prevent unintended fracture propagation and fluid migration. Accurately estimating this gradient is crucial to maintaining the integrity of both the disposal formation and adjacent geologic strata. Fracture pressure is one of the most important parameters in wellbore stability. It shows the rock's ability to hold vertical stress before starting to fracture. The application of fracture gradient (FG) affects the well design in areas such as the mud weight profile, casing setting depth, and cementing operation (Marbun 2015).

Based on injection pressure, volume, and time, pressure integrity tests are classified into three types: formation integrity test (FIT), leak-off test (LOT), and extended leak-off test (XLOT). Fracture pressure gradient can be determined using either direct or indirect methods. The direct method involves tests like LOT and FIT, while the indirect method calculates the gradient from logging data (Zhang and Yin 2017).LOT is a procedure in vertical wells where the well is shut in, and fluid/ water is injected into the well at a constant rate, gradually increasing the pressure.

At some point in the reservoir, the fluid will leak off and create a fracture, which can damage the well. In this method, the pressure breakdown directly measures the fracturing pressure.

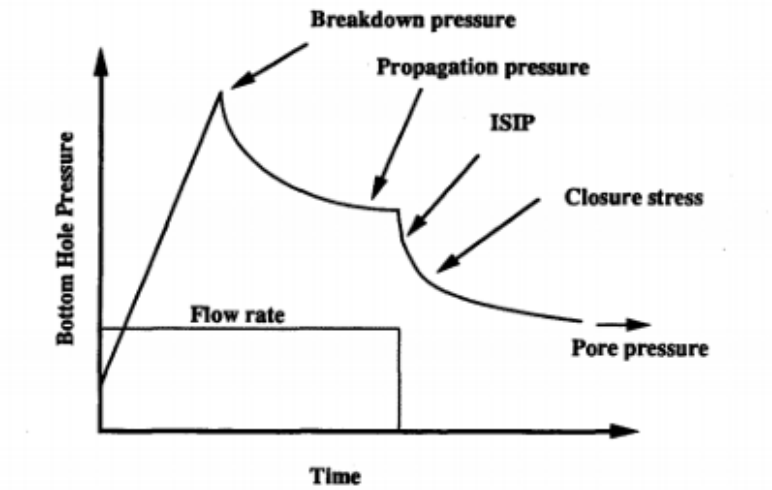


Figure 4-Fracturing and determination of the breakdown pressure from a leak off test. Adapted from (Wu 2017)

2.3.1. Understanding the mud losses while drilling

Zhang and Yin (2017) discuss how understanding the mechanism of mud losses during drilling can aid in better determining the fracture gradient. The possible causes of mud losses in drilling operations include seepage mud loss, small loss (occurring when mud pressure is greater than the fracture initiation pressure but less than the breakdown pressure), partial loss (occurring when mud pressure is slightly greater than the fracture breakdown pressure), and lost circulation. The methods for mud loss control and fracture gradient design vary for different cases. In most cases, the fracture gradient (FG) should be equal to or less than the breakdown pressure gradient (i.e., FG < Pb) to avoid uncontrollable mud losses.

2.3.2. Methods to predict the fracture gradient

- ***Hubbert–Willis. Hubbert and Willis***

The concept and calculation of fracture gradient probably first came from the minimum injection pressure proposed by Hubbert and Willis (1957), they assumed that the minimum injection pressure to hold open and extend a fracture is equal to the minimum stress:

$$P_{inj}^{min} = \sigma'_h + p = \sigma_h \tag{2.12}$$

Hubbert and Willis (1957) assumed that under conditions of incipient normal faulting, the effective minimum stress is horizontal and has a value of approximately one-third of the effective overburden stress, i.e., Therefore, they obtained the minimum injection pressure or fracture pressure in the following form:

$$P_{inj}^{min} = \frac{1}{3}\left(\sigma_v - p\right) + p \tag{2.13}$$

Where,

P_{inj}^{min} - minimum injection pressure,

σ_v - vertical stress

p - pore pressure.

Later, many empirical and theoretical equations and applications for fracture gradient prediction were presented.

- ***Matthews and Kelly Method***

Matthews (1967) presented a fracture gradient equation similar to Hubbert and Willi's equation. They introduced a variable “matrix stress coefficient” (ki), and they developed the concept of variable ratio between the effective horizontal and vertical stresses:

$$\frac{F}{D} = K_i\left(\frac{S}{D} - \frac{P}{D}\right) + \left(\frac{P}{D}\right) \tag{2.14}$$

The coefficient, Ki, relates the actual matrix stress conditions of the formation of interest to the conditions of matrix stress if the formation is compacted typically. Values for Ki are determined empirically from known fracture initiation pressures for an area (Wu 2017).

- ***Ben Eaton Method***

Eaton (1969) Used Poisson’s ratio of the formation to calculate the fracture gradient based on the concept of the minimum injection pressure proposed by Hubbert and Willis (1957):

$$\sigma_H = \frac{\nu}{1-\nu}\sigma_v \tag{2.15}$$

The resulting fracture gradient equation becomes –

$$\frac{F}{D} = \frac{\nu}{1-\nu}\left(\frac{S}{D} - \frac{P}{D}\right) + \frac{P}{D}$$

(2.16)

Eaton’s method enables considering the effect of different rocks (e.g., shale, sandstone) on fracture gradients because Poisson’s ratio considers the lithology effect.

2.4.Analytical vs. Numerical Approaches in Injection Volume Estimation

The selection for the appropriate modelling approach is very important for estimating the storage capacity of SWD reservoirs. Wu et al. (2023) discussed the influencing of the parameters of SWD capacity in a reservoir using a pot model. They concluded that the unknown extension of the aquifer area creates huge uncertainty in the storage capacity. For a reservoir with fixed volume, such as a hydrocarbon reservoir, the uncertainty range of the SWD capacity would be smaller as it is mainly affected by the total compressibility, even though the pore volume compressibility during pressurization would be much different from the depletion process When an aquifer has sensitive regions, such as faults and seismic monitoring regions, we often need to determine the pressure distribution in these regions before the SWD wells are placed. Wu (2017) discussed that a common challenge encountered during the water injection process is the decline in water injectivity over time. When the injection pressure exceeds the formation parting pressure, the reservoir may lead to undesirable consequences such as fault re-activation or fracturing, either inadvertently or intentionally. Understanding these dynamics is essential for optimizing water injection strategies and ensuring the long-term stability of the reservoir. It is also important to note that pore volume compressibility behaves differently during the reservoir pressurization compared to depletion which introduced us to the complexity in capacity predictions. These observations underscore the need for robust modeling frameworks. While numerical simulations offer a resolution, they are often data-intensive and very expensive. Ultimately, understanding the analytical and numerical approaches is essential for designing safe and effective injection strategies. Keeping in mind all the traditional methods, we have developed a more advance, easy-to-use, and robust model which is very user-friendly.

2.5.Pressure Superposition and its Effects on Injection Efficiency

For this composite model, Ramey (1970) developed a rigorous mathematical framework to analyze pressure transient behavior in reservoirs composed of multiple regions with distinct rock and fluid properties. This work is particularly important in cases where reservoirs exhibit heterogeneous characteristics, such as waterflooding operations, naturally fractured formations, and thermal recovery projects, where distinct zones exist with varying permeability, porosity, and fluid mobility. Ramey's study presents approximate analytical solutions for unsteady-state liquid flow in composite reservoirs by solving the diffusivity equation under conditions where reservoir properties change radially from the wellbore outward. The model considers radial composite reservoirs, which are divided into concentric zones, each with different properties such as permeability, porosity, and compressibility. The pressure and flow continuity at the interface between zones are rigorously maintained to ensure physical consistency. His approach provides a practical alternative to full numerical simulations, enabling engineers to predict pressure evolution in such reservoirs without resorting to computationally expensive models. The solutions illustrate how the storativity ratio and mobility contrast between different regions influence pressure drawdown and buildup responses.

We can apply this analytical approximation for a closed boundary to solve the problem above, as the method provides a useful tool for estimating reservoir parameters in well test analysis and history matching. By leveraging Ramey's framework, we can obtain first-order insights into the pressure behavior in composite reservoirs and assess key factors such as interface transmissibility and formation storativity contrasts, which are essential for production forecasting and reservoir management. Using Darcy's units, the pressure at an arbitrary location in the project area for a closed reservoir boundary is given by:

$$\frac{4\pi kh}{q\mu}\left[p_i - p(r,t)\right] = -E_i\left(-\frac{\phi\mu c_t r^2}{4kt}\right) + E_i\left(-\frac{\phi\mu c_t r_e^{\,2}}{4kt}\right) + \frac{4kt}{\phi\mu c_t r_e^{\,2}}\exp\left(-\frac{\phi\mu c_t r_e^{\,2}}{4kt}\right) \tag{2.17}$$

Where:

k – permeability

h – reservoir thickness

q – flow rate of the injection

μ - fluid viscosity

pi – initial reservoir pressure

p(r,t) – pressure at radial distance r and time t

φ – porosity

c_t – total compressibility

r – radial distance from wellbore

r_e – external boundary radius

t – time

Ei – exponential integral function

For a constant pressure outer boundary, the pressure distribution caused by a single well can be written as

$$\frac{4\pi kh}{q\mu}\left[p_i - p(r,t)\right] = -E_i\left(-\frac{\phi\mu c_t r^2}{4kt}\right) + E_i\left(-\frac{\phi\mu c_t r_e^{\,2}}{4kt}\right) \tag{2.18}$$

While for an infinite reservoir without external boundary, the pressure distribution caused by single well production/injection is:

$$\frac{4\pi kh}{q\mu}\left[p_i - p(r,t)\right] = -E_i\left(-\frac{\phi\mu c_t r^2}{4kt}\right) \tag{2.19}$$

The total compressibility is a linear combination of the pore volume compressibility and fluid compressibility stored in the pore volume.

As candidates for SWD, many aquifers or reservoirs may not have a reliable value for the pore volume compressibility. Many correlations can be applied in this case, and several are related to porosity and rock mineralogy (Ganat et al. 2024). It is worth pointing out that most correlations are from reservoir depressurization, while the SWD is a reservoir pressurization process. Wu et al. (2023) have pointed out that the magnitude of the pore volume compressibility for reservoir pressurization could be significantly different from (like to be larger) that of reservoir depressurization. In other words, the estimated capacity using these correlations might be much lower than the actual capacity given the same reservoir volume and pressure differential. In the case of missing porosity measurement, correlations between depth and porosity can be applied in the appraisal stage of SWD planning (Kim et al. 2018).

When we use these equations, we typically assign positive rates for production/extraction and negative rates for injection/disposal. If we have multiple wells in this region, pressure superposition can be applied to solve the pressure at the point of interest (Ganjdanesh and Hosseini 2018). The equations for multiple wells with a mix of injections/production are shown below in the Appendix.

2.6.Uncertainty Analysis incorporated in this model

Since there are huge uncertainties with the parameters used in the geomechanics model, especially for SWD into several formation intervals with perforation intervals up to 1000+ ft, any deterministic results without probability can't be used confidently without concerns about fracturing. To overcome this problem, we suggested and discussed the application of stochastic

modeling, such as Monte Carlo (MC) simulations as supported by previous works (Jing and Wu 2019, Wu et al. 2023).

In this paper, we apply the MC simulation with the Latin hypercube sampling (LHS) (Shields and Zhang 2016, Iman 2008). LHS is an advanced stratified sampling technique designed to improve the efficiency and robustness of MC simulations, particularly in high-dimensional spaces. Unlike simple random sampling, LHS divides each input variable's probability distribution into N equally probable intervals and then ensures that each interval is sampled exactly once, which guarantees a more uniform and comprehensive exploration of the entire parameter space. This systematic partitioning reduces the clustering of samples and the risk of missing extreme values, thereby lowering the variance of simulation outcomes and improving the precision of uncertainty and sensitivity analyses. As a result, LHS often requires fewer simulation runs to achieve statistically significant results compared to traditional MC methods, making it particularly useful in complex modeling scenarios such as risk assessment, engineering design, and environmental forecasting. The method's ability to capture the full variability of inputs with a reduced computational burden makes it an indispensable tool for robust simulation studies.

In the petroleum industries where the decision often relies on incomplete data and high investment risks, a solution for this is necessary. Over the years, traditional analytical approaches that rely on fixed parameters have undergone substantial evolution. The introduction of stochastic variables, commonly encountered in the oil industry, has become increasingly practical for addressing a wide range of challenges. This transformation is largely driven by the adoption of Monte Carlo techniques, which provide a cost-effective means to evaluate uncertainties and enhance decision-making processes(Stoian 1965).

Moreover, different geomechanical and mathematical models that are used in the well stability studies, do not include the uncertainty assessments of the models. As the majority of input

parameters into the geomechanical models are subjected to some extent of errors and uncertainties, therefore, it is essential to quantify the uncertainty associated with the output of the geomechanical models (Tabatabaee Moradi and Nikolaev 2020).

Monte Carlo analysis is applied to estimate the range of possible fracturing pressures, considering the natural variability in several key input parameters. These inputs include reservoir petrophysical and geomechanical characteristics, the quality of the injected fluid, well specifications, and tubing configurations.(Aamri et al. 2017) used a semi-analytical wellbore equation to predict a range of bottom-hole pressure used to avoid fracturing in carbonate and shale formations and then validated it by probabilistic results using the Monte Carlo Analysis. The analysis yields essential calculations such as the injection pressures at both the bottom hole and wellhead, overall, well injectivity, and whether the injection occurs within the formation matrix or causes fracturing. For injections resulting in fracturing, additional fracture characteristics are assessed, including fracture length, net pressure within the fracture, and fracture skin.

In the developed model, pressure variations resulting from changes in pore pressure are represented through the poroelastic coefficient, defined by:

$$A_p = \beta\alpha \frac{1-2\nu}{1-\nu} \tag{2.20}$$

Where,

- β is the Perkins and Gonzalez shape factor,
- α is Biot's poroelastic parameter, and
- ν is Poisson's ratio.

The shape factor β, derived from Perkins and Gonzalez's work, describes the area of the reservoir impacted by fluid injection and temperature changes. This factor ranges from:

- 0 (when only a small region on each side of a fracture experiences cooling),

- to 0.5 (when a minor radial distance from the wellbore is cooled),

- to 1.0 (when cooling extends such that the thermal front surpasses the formation height or the half-length of a fracture).

Similarly, the thermoelastic coefficient is given by:

$$A_t = \frac{\beta E \alpha_t}{1 - \nu} \tag{2.21}$$

where:

- E is Young's Modulus, and

- αt is the coefficient of linear thermal expansion.

These coefficients allow the model to capture both poroelastic and thermoelastic effects within the reservoir enhancing the fracture risk assessment and operational planning.

2.7.Summary of Research Opportunities

Most models, existing today rely on complex numerical simulations which also ignore the geomechanical factors such as poroelastic and thermoelastic stress effects, which is critical in injection scenarios. Numerical simulations require detailed sub-surface data which is not always available or economically feasible to obtain. Many models have failed to address the pressure interactions between multiple injection and extraction wells in reservoirs particularly under varying boundary conditions. Without the uncertainty, the predictions made for the fracturing pressure and injectivity can be misleading and unsafe sometimes. These gaps highlight the need for a practical, efficient, and easy-to-use model that incorporates pressure superposition, geomechanical constraints, and probabilistic forecasting. The analytical model proposed in this study addresses these issues, offering a tool to estimate the safe injection volumes and supporting SWD planning under any uncertainty.

3. Methodology

3.1. Analytical solution to predict the pressure in a reservoir with multiple production/injection wells

We first introduce the concept of a project area containing multiple production and injection/disposal wells. From the database (Enverus as an example), the production and injection history and well data can be obtained, including longitudes and latitudes, true vertical depth, and thickness. The project area is related to the reservoir, is shown in Figure 5.

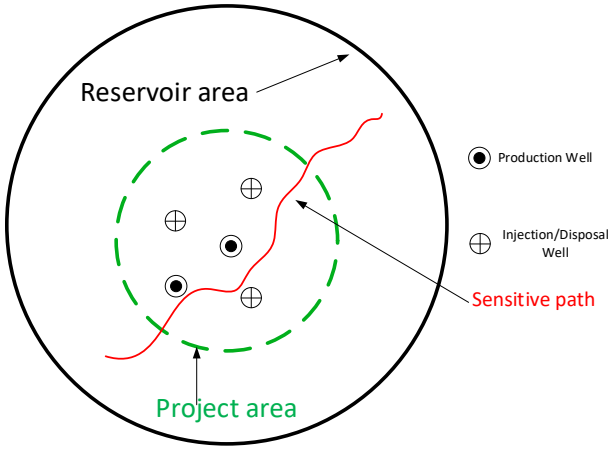


Figure 5-The concept of project and reservoir areas with multiple wells

In the development, the external reservoir boundary condition can be an open boundary with constant pressure, closed boundary, and infinite acting. Furthermore, we have made the following assumption for this model:

- The reservoir has a uniform thickness, porosity, and permeability.
- We ignore the wells and well activities outside the project area.
- Fluids inside the reservoir are slightly compressible, as are Newtonian fluids.
- Fluid flow satisfies the Darcy's law.

- The initial pressure is constant across the reservoir.

While it is trivial to know that the average reservoir for an infinite reservoir will be the initial reservoir pressure, the solutions for closed-boundary and open-boundary reservoir conditions are reviewed in section 2.5.

3.2. Applied geomechanical model in this research

We applied two geomechanical models to capture both poroelastic and thermoelastic effects within the reservoir. The first model presented by Jing and Wu (2019) as this model is cast as:

$$\sigma_{frac} = \sigma_0 + \xi A_p\left(p_i - p_e\right) + A_t\left(T_i - T_0\right) \tag{3.1}$$

The poroelstic factor A_p is defined in Eqn (2.20) and the thermoelastic coefficient A_t is given in Eqn (2.21). In the modeling effort, we also applied another model introduced by Hosseini et al. (2014). The equation was formulated to estimate the fracture pressure by considering the rock and the geomechanical properties. Factors like saturated rock density, Biot's coefficient, Poisson's ratio, stress ratio, thermal expansion, temperature drop, and Young's modulus were incorporated in the equation which can be used in both normal and reverse faulting stress regimes.

$$P_{frac} = \frac{1}{\left[2\alpha - \beta_v - \beta_h - \left(\beta_v - \beta_h\right)\cos 2\theta + \frac{\left(\beta_v - \beta_h\right)\sin 2\theta}{\mu}\right]} \cdot \begin{bmatrix} \left\{(1+K)+(1-K)\cos 2\theta - \frac{(1-K)\sin 2\theta}{\mu}\right\}\sigma_{v0} \\ -\left\{\left(\beta_v + \beta_h\right)+\left(\beta_v - \beta_h\right)\cos 2\theta - \frac{\left(\beta_v - \beta_h\right)\sin 2\theta}{\mu}\right\}P_0 \\ \frac{-2\alpha_t E \Delta T}{1-2\nu} \end{bmatrix}$$

(3.2)

and

$$P_{frac} = \frac{1}{\left[2\alpha - \beta_h - \beta_v - \left(\beta_h - \beta_v\right)\cos 2\theta + \frac{\left(\beta_h - \beta_v\right)\sin 2\theta}{\mu}\right]} \cdot \begin{bmatrix} \left\{(K+1) + (K-1)\cos 2\theta - \frac{(K-1)\sin 2\theta}{\mu}\right\}\sigma_{v0} \\ -\left\{\left(\beta_h + \beta_v\right) + \left(\beta_h - \beta_v\right)\cos 2\theta - \frac{\left(\beta_h - \beta_v\right)\sin 2\theta}{\mu}\right\}P_0 \\ \frac{-2\alpha_t E \Delta T}{1-2\nu} \end{bmatrix} \quad (3.3)$$

where,

α - Biot's poroelastic constant

ν - Poisson's ratio

K - Initial total horizontal-to-vertical ratio for normal and reverse faulting stress regimes

α_t - Coefficient of linear thermal expansion

ΔT – Temperature difference between injection temperature and reservoir temperature

E - Young's Modulus

β_v and β_h are the stress coupling ratios for the infinite homogenous medium, which can be calculated by –

$$\beta_h = \frac{\Delta\sigma_h}{\Delta P} = \frac{\Delta\sigma_H}{\Delta P} = \frac{\alpha(1-2\nu)}{(1-\nu)} \quad (3.4)$$

and

$$\beta_v = \frac{\Delta\sigma_v}{\Delta P} = \frac{\left(\frac{\alpha}{2}\right)(1-2\nu)}{(1-\nu)} \quad (3.5)$$

To improve the predictability of injection performance and mitigate potential risks, future research should prioritize coupled thermo-hydro-mechanical-chemical (THMC) modeling approaches that incorporate temperature-dependent rock properties, dynamic stress evolution, and long-term geochemical interactions. Field-based monitoring techniques, such as fiber-optic distributed temperature sensing (DTS) and microseismic monitoring, can further enhance the understanding of temperature-induced stress alterations and help validate numerical models.

3.3. Determining the Maximum Injection Capacity for a Reservoir

While the maximum injection capacity for the cases of infinite reservoir boundary and constant external pressure would be infinite, it is only meaningful when we talk about the maximum water disposal volume for the case of the closed boundary. Using the concept of reservoir storage capacity introduced in the literature(Wu et al. 2023), we have

$$\delta = c_t\left(p_{\max} - \bar{p}\right) \tag{3.6}$$

where

$c_t = total\ compressibility, \frac{1}{psi}$

$p_{max} = maximum\ reservoir\ pressure, psi$

$\bar{p} = average\ reservoir\ pressure, psi$

The water storage capacity is a dimensionless variable describing how much water can be stored per unit pore volume in a closed aquifer/reservoir. The average reservoir can be estimated either from the material balance or the volumetric average in the reservoir as follows. For example, we can calculate the average pressure in the project area by dividing the area into multiple grid blocks, and each grid block has a volume of dV, then the average reservoir pressure is

$$\bar{p} = \frac{\int_0^{V_{PA}} p dV}{V_{PA}} \tag{3.7}$$

Where: V_{PA} is the reservoir bulk volume in the project area. If each grid has the same volume, then the average pressure is the arithmetical average of the pressure at the center of the gridlock. This can be conveniently solved by the pressure superposition discussed above.

We also need to determine the maximum allowable injection pressure from the reservoir storage capacity concept. Wu et al. (2023) discussed two scenarios where maximum pressure should be determined for the SWD operations. One is the maximum injection pressure without fracturing the reservoir formation; and the other one is the other one is the pressure controlling the fault re-activation.

3.4.Case Study to Predict Pressure Distribution and Maximum Injection Capacity

This study comprehensively evaluates a mature hydrocarbon-producing region, utilizing production and injection history data to estimate average reservoir pressure and forecast maximum injection capacity for saltwater disposal. The primary objectives of this study are: (1) to characterize the reservoir using available historical well data, (2) to estimate current reservoir pressure based on pressure superposition techniques, (3) to statistically analyse key reservoir properties, and (4) to forecast maximum sustainable injection capacity using MC simulation. The selected region comprises 274 wells completed in the layer of our injection target interval, including plugged and abandoned (P&A) wells, active producers, and injection wells, with operational histories from the 1940s to 2024. The well locations and status at the end of 2024 is shown in Figure 6. We used about 200 wells for reservoir characterization after filtering out horizontal and directional wells. The porosity is calculated from true vertical depth, and the pore volume compressibility is calculated using porosity. Their distributions are

shown in Figure 7. The average properties are used to estimate the other reservoir parameters as shown in Table 1.

The methodology follows a structured approach: (1) Data Collection and Preprocessing – assembling and standardizing historical production, injection, and pressure data; (2) Reservoir Characterization – computing statistical distributions of porosity, net thickness, and pressure; (3) Pressure Estimation – applying pressure superposition techniques to determine the current average reservoir pressure; (4) Maximum Injection Capacity Forecasting – developing a probabilistic model using MC simulation to estimate injection limits under different operational scenarios while accounting for geological and operational uncertainties.

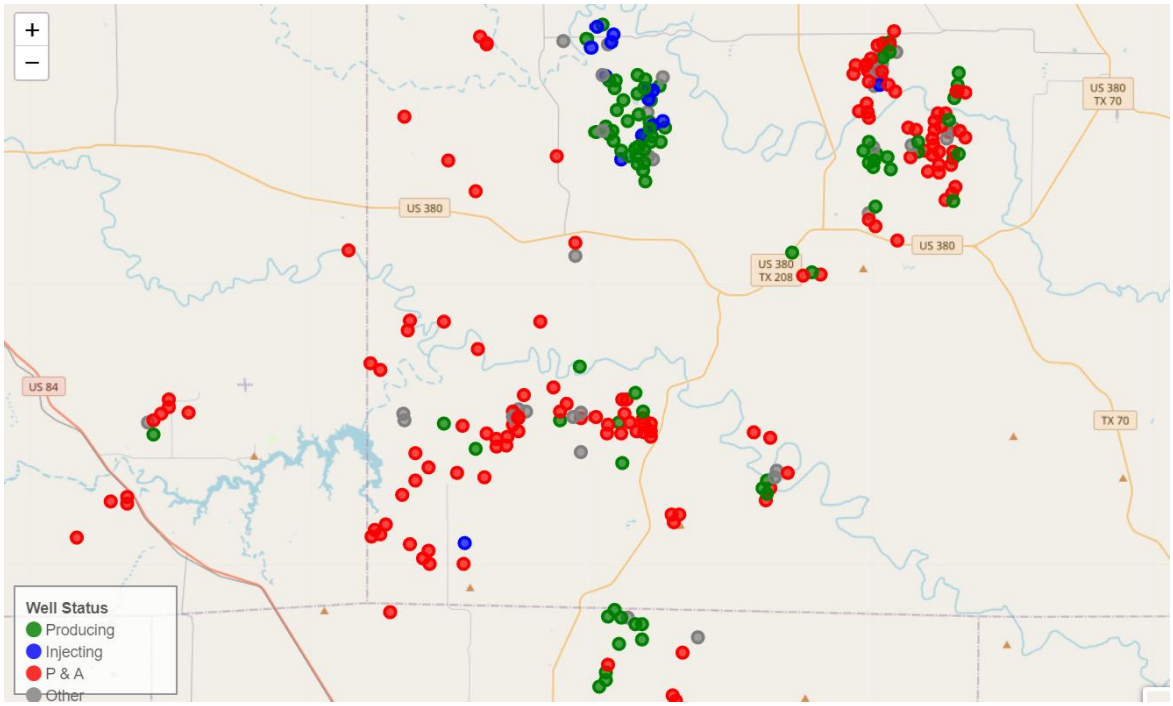


Figure 6-Wells in the project region. The project area is around 150,000 acres with 274 wells

Table 1: Average properties of the reservoir characterization in the project area from the well data.

Property	Value	Unit
Depth	7053.7	feet
Net thickness	62.9	feet
Initial pressure	3174.17	psi
Reservoir Temperature	118.7	F
Porosity	0.213	fraction
Permeability	168.357	mD
Total compressibility	5.91E-06	1/psi
Unit pore vol	1.0E+05	BBL/Acre
Storativity	0.616	BBL/Acre/psi

We further assume that the reservoir is 10 times the region covered by the wells. Then we applied the pressure superposition algorithms discussed earlier. The pressure heat map is shown below with an average reservoir pressure of 2933 psi at the end of injection history. We applied the MC simulation with the LHS algorithm in determing the fracturing pressures given that the target interval is over 350+ ft net pay.

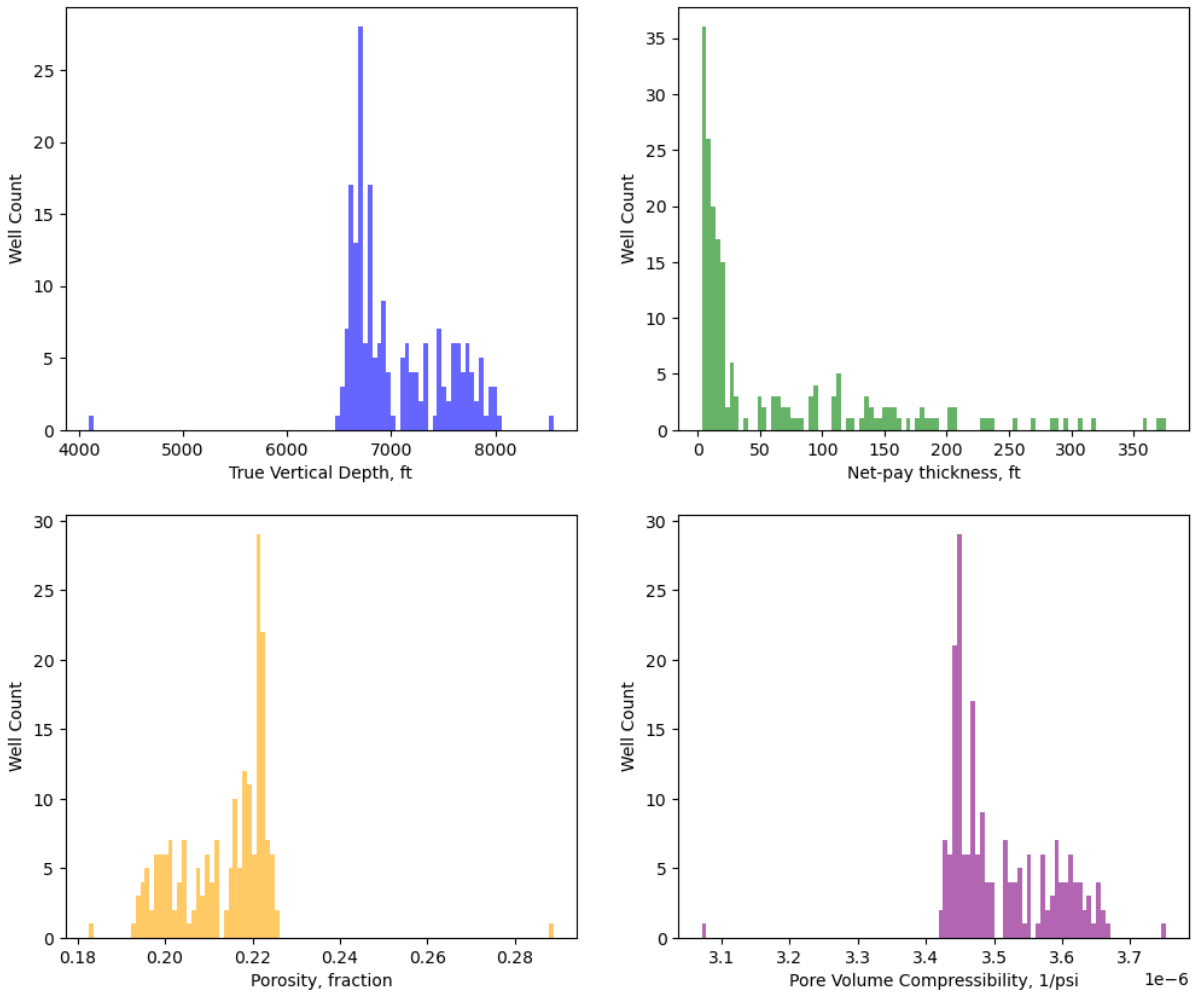


Figure 7- Histograms showing the frequencies of reservoir properties. True vertical depth and net-pay thickness are from well database, and porosity, pore volume compressibility are calculated from correlations.

The analysis uses the pressure superposition principles, which enable the reconstruction of historical pressure evolution and estimate the current average reservoir pressure by integrating historical well performance and injection/withdrawal rates. Some geological features will only be hypothetically added to enhance visualization and analysis for illustration purposes.

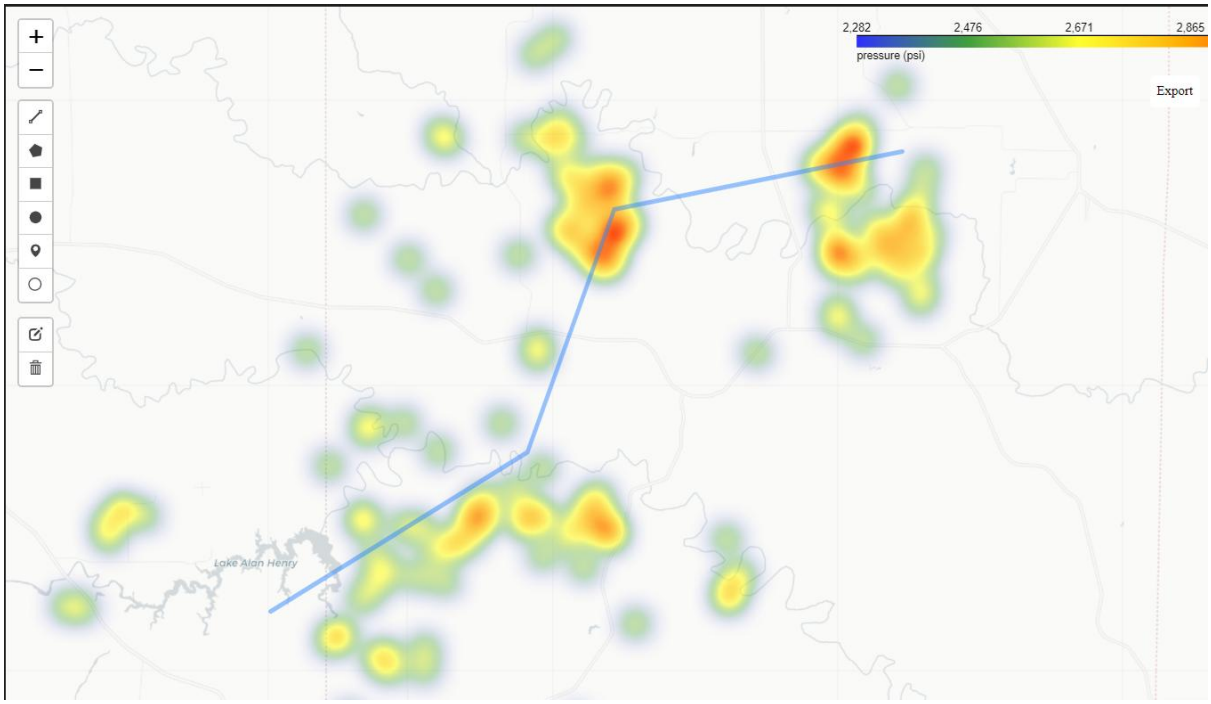


Figure 8-Pressure heat map in the project area calculated by pressure superposition of all wells. The blue multi-segment line is a hypothetical pressure sensitive region for reservoir surveillance.

Suppose the multi-segment blue line represents a pressure-sensitive region, and we want to monitor the pressure along this path. With pressure superposition algorithms, the pressure distribution at any time of interest, or future forecast can be achieved readily.

To determine the maximum injection capacity distribution, one needs to calculate the maximum pressure allowable for injection first. The maximum pressure can be the pressure in the pressure sensitive region, or the fracturing pressure of the rock. Here we used the fracturing pressure as an example, and with 8000 realizations, we obtained the fracturing pressure distribution in this region.

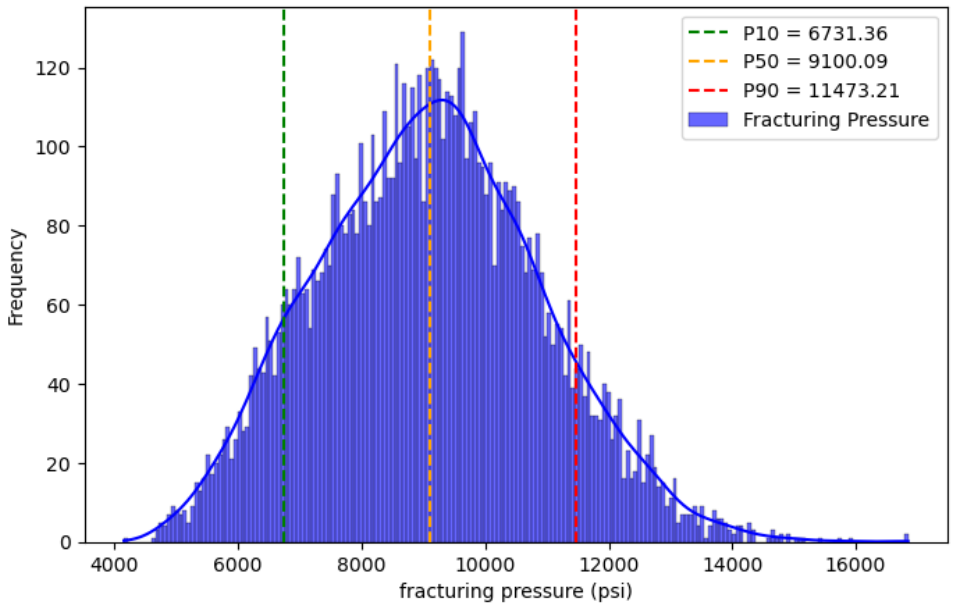


Figure 9-Distribution of fracturing pressure for the formation interval in the project area using MC simulation with LHS algorithms. P10 means the probability of fracturing pressure less than 6731 psi is less than 10%.

The additional injection volume before the pressure reaches the fracturing pressure is

$$Q = 0.007758 A h_{net} \phi \delta \tag{3.8}$$

Where Q is the additional SWD volume in this area in MMSTB, A is the area in acres, h_{net} is the net pay thickness here, we assume it is the perforation interval length, porosity is determined by the well's true vertical depth, and δ is aquifer storativity.

Since the average pressure has been determined, the area is given, and the distributions for net pay thickness, porosity, and total compressibility are calculated from the properties of 200 wells. With these, we can determine the distribution of the additional injection volume, as shown below-

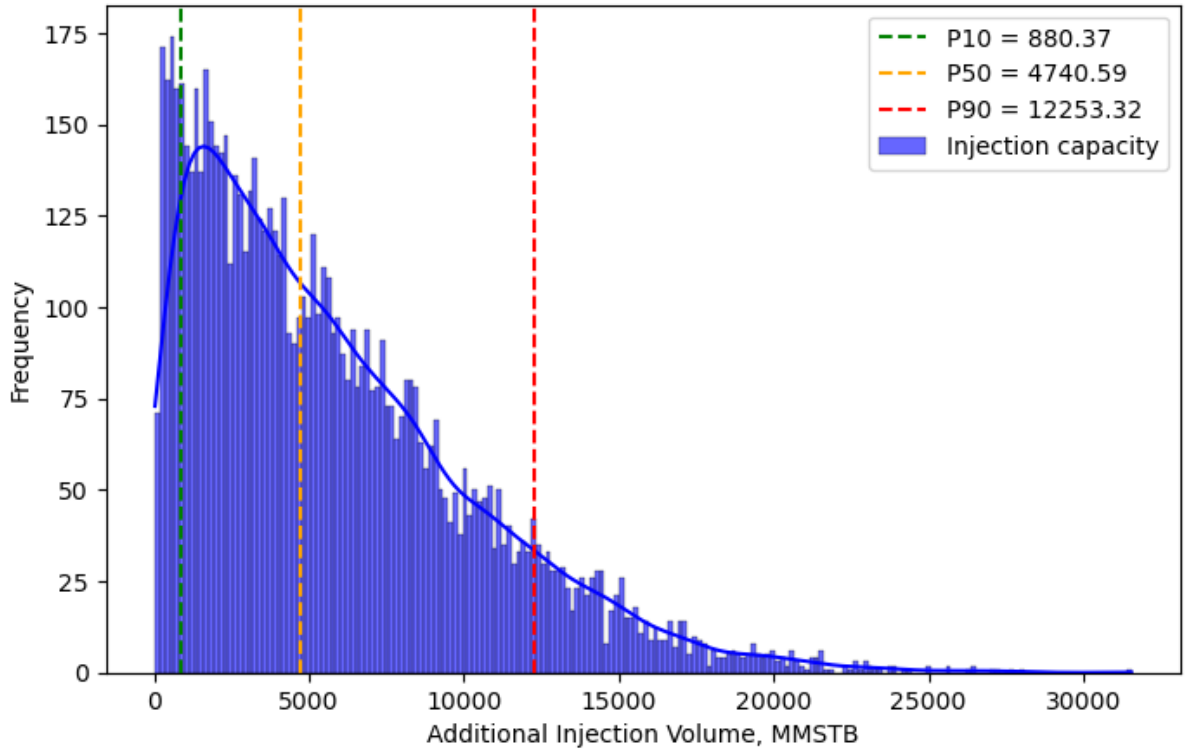


Figure 10-Distribution of additional injection volume before the rock fails in the project area.

This study provides a robust framework for optimizing saltwater disposal strategies in mature oil and gas fields while ensuring formation integrity and regulatory compliance by integrating historical data analysis, statistical reservoir characterization, and probabilistic modeling. The results will aid long-term injection planning and support decision-making for enhanced wastewater management in similar reservoir settings.

3.5.Determination of well injectivity before and after the fracture formation

The injection of water for pressure maintenance and waterflooding applications or the disposal of produced water are becoming increasingly important issues in managing produced fluids(Sharma et al. 1997).Well injectivity (J) is a useful measure of the effect of plugging and formation damage on injection well performance. The half-life of an injection well is defined as the time required for its injectivity to decline to half its initial value(Saripalli et al. 2000)

The injectivity of a well that measures the ability of an injection well to receive injected fluid can be defined as the following –

$$J = \frac{Q}{P_{wf} - P_e} = \frac{kh}{141.2\mu B\left(\ln\frac{r_e}{r_w} + s\right)} \tag{3.9}$$

Where Q is the flowrate at standard conditions measured in STB/day

P_e – external boundary radius pressure, psi

P_{wf} -bottom hole flowing pressure, psi. ‘

R_w-wellbore radius, ft

s-total skin factor

While the fracture grows into the reservoir, the well injectivity is improved, restoring the initial injectivity index. This phenomenon must be included in the injectivity index calculation through the geometrical factor, which calculates the formation damage factor due to fracture, sf. There are models to calculate the formation damage factor for hydraulic fracturing after a stimulation procedure, but there are no exclusive models to use with fractures induced by water injection. In a fractured regime, the injectivity of a well can be defined similarly (Wu 2017). Calculating the formation damage factor for hydraulic fracturing is very critical; this can be calculated by introducing the fracture dimensionless conductivity, which is,

$$C_{fD} = \frac{k_f w}{k x_f} \tag{3.10}$$

In cylindrical coordinates the pseudo-steady-state flow equation for a hydraulically fractured oil well is –

$$q = \frac{kh\left(\bar{p} - p_{wf}\right)}{141.2B\mu\left[\ln\frac{r_e}{r_w} - 0.75 + s_f\right]} \tag{3.11}$$

Thus, the flow equation and injectivity index could be calculated-

$$r'_w = r_w e^{-sf} \tag{3.12}$$

$$r'_w = \frac{x_f}{\frac{\pi}{C_{fD}} + 2} \tag{3.13}$$

Using the concept of equivalent radius as mentioned in Eqn (3.13), the skin factor can be calculated.

3.6.Relationship between Injection Pressure and Injection Rate

In the process of water injection deployment application, problems often occur due to the influence of the injected water quality, reservoir pressure, nozzle flow resistance, nozzle clogging, and the difficulty in achieving reasonable flow allocation(Li et al. 2024).

Critical parameters like surface pump pressure and injection rate are typically known in an injection process. These helps determine whether the injection pressure exceeds the formation's parting pressure, allowing us to assess whether the water is injected through a fracture or directly into the formation matrix.

To interpret injection data accurately, we must understand the formation face's bottom hole pressure (BHP). BHP is influenced by several factors: surface pump pressure, pressure drop due to friction along the tubing, hydrostatic head, and any pressure drop caused by the completion system in place. The pressure changes along the injection string (either through

tubing or annulus) depends on potential energy, kinetic energy, and friction. Kinetic energy effects can typically be ignored, except in high flow rates or specific restrictions.

In a simplified case of single-phase flow, without considering acceleration effects, BHP at the formation face can be calculated using surface pressure as follows:

$$BHP = P_{surface} + P_{hydrostatic} - P_{friction} \quad (3.14)$$

Where:

- BHP is the bottom hole pressure at the formation face, measured in psi,
- P_surface is the surface pressure in psi,
- P_hydrostatic is the hydrostatic pressure from the fluid column in psi and
- P_friction is the frictional pressure drop through the tubing, completion, and perforations in psi.

This formula helps estimate the bottom hole pressure by accounting for each contributing pressure change from the surface to the formation face. In sections below, we will study how to determine these factors.

3.6.1. Determination of friction in the injected string (P_friction)

When modeling steam flow in wellbores, the effect of friction work on the temperature/steam quality of both fluids in wellbores and reservoirs should be considered (Sun et al. 2018).

Sun et al. (2018) suggestions for energy balance equations for steam flow in inner tubing (IT) and annuli are developed, considering the effect of friction work on the energy re-distribution process in the system.

In modern fracturing treatments, friction loss in the pipe has often been the limiting factor in obtaining the high injection rates desired for maximum effectiveness (Ousterhout and Hall 1961).

The frictional pressure drop along the tubing per unit length is calculated with the following expression:

$$\frac{dP}{dL} = 0.3813 \frac{f \rho q^2}{D^5} \tag{3.15}$$

Where:

-DP is the pressure change (in psi),

- dL is the length over which the pressure drop is measured (in feet),

- f is the Moody friction factor (dimensionless),

- ρ is the fluid density (Lb_m/ft^3),

- q is the injection rate (in barrels per minute, BPM), and

- D is the diameter of the tubing (in inches).

As fluid flows through the tubing, energy losses occur due to friction. These losses are usually irreversible and cannot be accurately predicted for turbulent or transitional flows. A friction factor is introduced to address this, which helps account for these energy losses (Wu 2017).

The friction factor f varies based on the flow regime and is linked to the Reynolds Number, which characterizes flow behavior. The Reynolds Number (Re) is calculated by:

$$Re = 7737.6 \frac{D \times \nu \times \gamma_g}{\mu} \tag{3.16}$$

Where:

- Dis the tubing diameter (in inches),

- v is the fluid velocity (ft/s),

- γ_g is the fluid's specific gravity and

- μ is the fluid’s viscosity (in centipoise).

The flow regime determines how friction is affected by factors like surface roughness. For example, in laminar flow (Re < 2100), friction is not affected by roughness, and f is calculated by:

$$f_M = \frac{64}{N_{Re}} \tag{3.17}$$

In turbulent flow (Re > 2100), f is more complex and can be calculated using the Colebrook-White equation:

$$\frac{1}{\sqrt{f_M}} = 1.74 - 2\log\left(\frac{2\varepsilon}{D} + \frac{18.7}{N_{Re}\sqrt{f_M}}\right) \tag{3.18}$$

This study uses these equations to account for frictional losses across different flow conditions, helping to ensure accurate pressure drop estimates in various flow regimes.

3.6.2. Bottomhole pressure and hydrostatic head pressure

We start by calculating the frictional pressure drop along the tubing to calculate bottom hole pressure from surface pressure. After that, the hydrostatic head is determined.

For a liquid, the hydrostatic pressure (or static bottom hole pressure) is obtained by multiplying the fluid gradient by the actual vertical depth (TVD):

$$P_{hydrostatic} = TVD \times gradient \tag{3.19}$$

The fluid gradient itself can be calculated based on the fluid's specific gravity (γ_g) as follows:

$$gradient\left(\frac{psi}{ft}\right)=\frac{\gamma_g\times 62.4}{144}=\gamma_g\times 0.433 \tag{3.20}$$

This formula allows us to estimate the pressure exerted by the fluid column down to the bottom hole, providing an accurate means to convert surface pressure to bottom-hole pressure in liquid injection scenarios.

3.6.3. Determination of surface pressure

The viscosity of injection water is determined by a correlation that considers temperature, pressure, and the total dissolved solids (TDS) in the water.

For specific gravity, the following correlation is used, incorporating TDS and temperature (T) effects:

$$\gamma_g=\left(7.572\times 10^{-3}TDS+0.998238\right)\times 1.002866e^{\psi}$$

$$\psi=3.0997\times 10^{-6}\left(\frac{P_i+P_{wellhead}}{2}\right)-2.2139\times 10^{-4}\left(T_i-59\right)-5.0123\times 10^{-7}\left(T_i-59\right)^2 \tag{3.21}$$

Where:

- TDS is the percentage of total dissolved solids,
- T is the injection water temperature (°F),
- P is the pressure (psi), and
- ψ adjusts specific gravity based on pressure and temperature.

Specific gravity varies with temperature and TDS concentration. Using specific gravity, the hydrostatic pressure at any depth (z) can be calculated by:

$$P_{hydrostatic}=0.433\times z_{datum}\times\gamma_g \tag{3.22}$$

This approach provides a practical way to estimate hydrostatic pressure based on water properties under injection conditions. Water has consistent properties (density, viscosity, etc.), which can simplify the calculation compared to more complex fluids like oil or multiphase mixtures.

3.7.Validation of Analytical model through numerical model results

This study used a computational approach to develop a numerical model simulating water injection operation in a closed reservoir system. This model evaluates the pressure distribution, fluid flow and the maximum allowable pressure to ensure it does not fracture the well .

To construct the numerical model, a structured cartesian grid was used with a reservoir size of 10x10 km containing 16 equally spaced water injection wells as shown in Figure 2. The grid resolution was selected to balance the efficiency and the accuracy of the pressure variations. The input parameters for the reservoir and the fluid properties used in this case study are shown in table 2.

Table 2 - Reservoir properties

Properties	Values
Grid blocks	100*100*1
Initial pressure, Psi	3,500
Reservoir temp, F	130
Porosity	0.2
Permeability, mD	100
Rock compressibility,1/Psi	3.0E-6
Maximum injection pressure, psi	8,000
Reservoir area, km2	100
Boundary condition	closed

The model was initialized with an initial pressure of 3,500 psi and a water injection rate of 3,000 bbl/day per well. The simulation was run for 15 years, during which the pressure buildup was monitored to determine the maximum allowable pressure. Key assumptions made in the numerical model are

- Isothermal conditions were assumed throughout the simulation
- The reservoir was homogeneous.
- No-flow boundaries were applied to simulate a confined area
- Water was injected at a constant rate to observe the pressure distribution

The results revealed an increase in bottom-hole pressure over time with pressure accumulation near the injection as shown in Figure 12. The maximum bottom-hole pressure reached 8,300 psi, remaining within the safe limits. Similar approaches have been employed in previous studies, where numerical modeling was used to assess reservoir injectivity under varying geomechanical conditions, such as Smith & Brown (2019), which highlighted the impact of formation permeability on pressure evolution. These studies support the methodology adopted in this case study, reinforcing the reliability of numerical predictions.

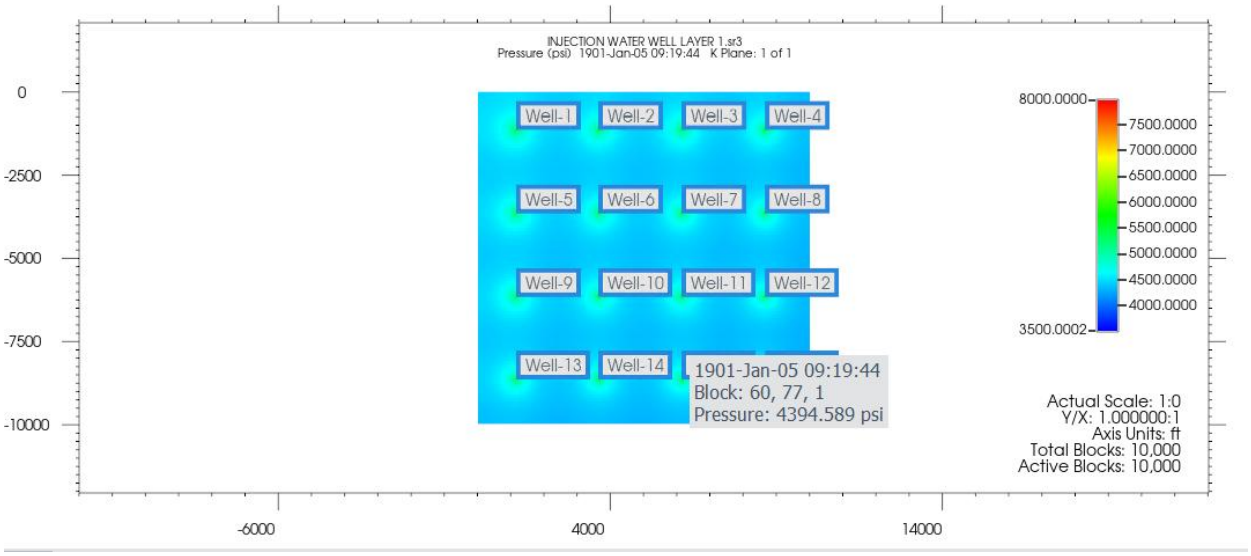


Figure 11-Pressure display after 15 years of water injection estimated by numerical modeling

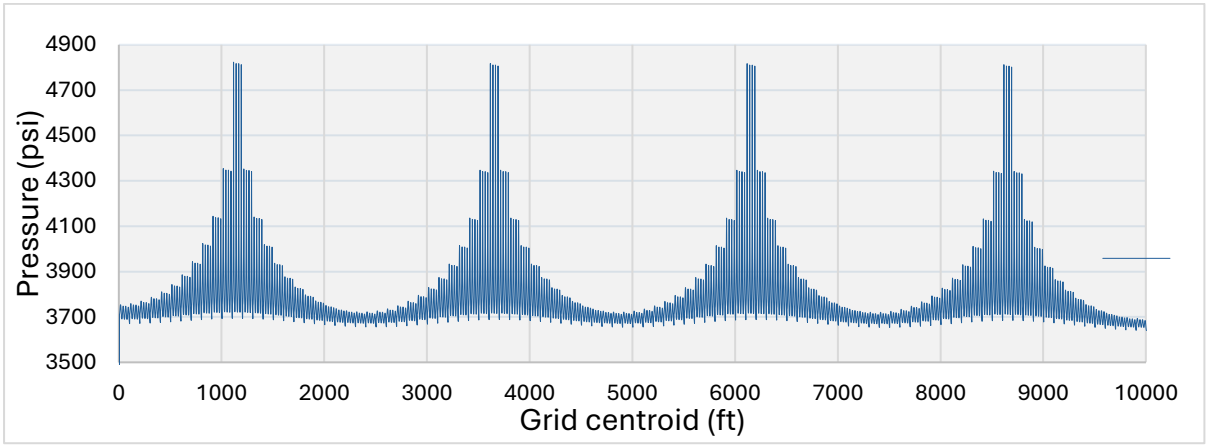


Figure 12- Graphical representation of pressure spikes near the injection point

As shown in Figure 12, the observed pressure increase suggests the multiple injection well where the fluids is introduced into the reservoir. The pressure behavior follows the pressure superposition principle.

The pressure distribution can be expressed using Eqn 2.17.

The sharp pressure spikes around injection wells occur due to:

1. Immediate response to fluid injection: When fluid is injected into a formation, pressure builds up rapidly at the injection point.
2. Superposition effect: If multiple wells exist, pressure responses from each well add up in overlapping regions, modifying the local pressure distribution.
3. Formation and grid effects: The pressure distribution depends on the rock permeability, porosity, and computational grid resolution.

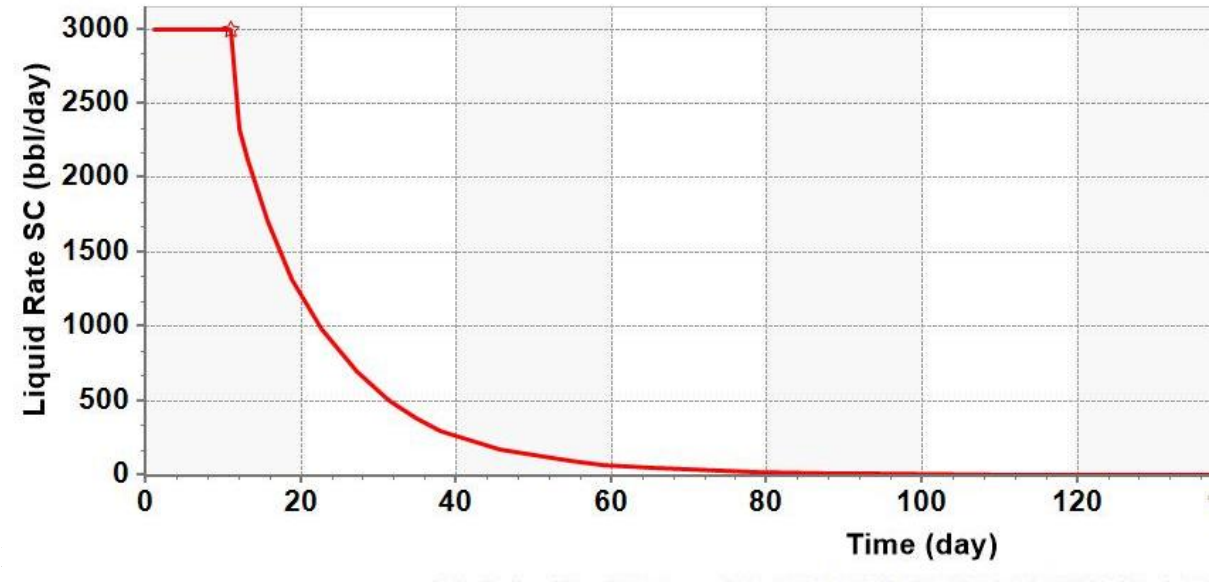


Figure 13- Graphical representation of liquid rate in standard conditions vs the time in days

The pressure response observed in the numerical model closely follows the principle of pressure superposition, supporting the theoretical foundations of the analytical model.

4. Results and Conclusions

4.1.Future Work

While this research has provided valuable insights into estimating the maximum injection volume for reservoirs using an analytical model, there remain opportunities for further development and exploration. Future work can enhance the current model's applicability and accuracy by incorporating additional factors and refining existing assumptions. One significant area for improvement is the incorporation of complex geomechanical behavior. The current model assumes simplified geomechanical properties, but future studies could integrate more comprehensive models that account for anisotropy, stress field variations, and dynamic changes in rock properties during injection operations. Additionally, expanding the dataset for model validation using field data from various geological settings and operational scenarios would improve the robustness and reliability of the model. Collaborations with industry partners could provide access to real-world data for further validation.

Furthermore, additional probabilistic methods and sensitivity analysis could be employed to better quantify model uncertainty and assess the impact of individual parameters. While the current study includes uncertainty analysis using Monte Carlo simulations, further refinement in this aspect would enhance the reliability of model predictions. The model could also be extended to evaluate reservoir performance in other applications, such as geothermal energy production, CO2 sequestration, and underground gas storage, with further modifications tailored to the specific requirements of these applications.

In conclusion, future research focusing on these areas will contribute to the continuous improvement of reservoir management practices. By enhancing the accuracy and applicability of the analytical model, stakeholders can make more informed decisions in maintaining reservoir integrity and optimizing injection operations.

4.2.Conclusions

Effective SWD well design and management require a multi-disciplinary approach involving reservoir engineering, geomechanics, and regulatory compliance to achieve safe and efficient injection operations. By proactively addressing pressure limitations, injection capacity constraints, and formation integrity concerns, operators can enhance long-term injection performance, minimize regulatory risks, and ensure sustainable wastewater disposal in oil and gas operations. While extensive modeling efforts have been conducted to account for the interplay between in-situ stresses, poroelasticity, and fluid-rock interactions, the influence of temperature variation remains relatively less studied and poorly understood in practical SWD applications. Most existing models primarily focus on isothermal conditions or employ simplified assumptions regarding the thermal impact on stress fields. However, recent studies suggest that thermal effects can significantly influence fracture propagation, stress redistribution, and long-term reservoir compaction, necessitating a more integrated approach to SWD well design.

This study shows that factors like in-situ stress, rock properties, and volumetric properties are the major factors that can affect the fracturing pressure for formation. In this study, different methods are used to validate the results of the analytical method. Monté Carlo simulations are used to understand the range of uncertainties in the formation. This study presents an analytical approach to estimating the maximum injection capacity of saltwater disposal (SWD) reservoirs while integrating geomechanical considerations and historical production/injection data. The proposed methodology leverages pressure superposition principles to estimate average reservoir pressure, incorporates geomechanical constraints to determine fracturing pressure, and employs Monte Carlo simulations to quantify uncertainty in injection capacity predictions. The following key conclusions are drawn:

1) Reservoir Pressure and Injection Capacity Estimation

• The application of pressure superposition effectively reconstructs historical pressure distribution and provides an accurate estimation of current reservoir pressure in multi-well SWD operations.

• By integrating statistical reservoir characterization, key reservoir properties such as porosity, permeability, and total compressibility were determined and incorporated into the injection capacity forecast.

2) Geomechanical Constraints on Maximum Injection Pressure

• The fracturing pressure of the target formation was estimated using poroelastic and thermoelastic stress models, considering in-situ stress conditions, thermal effects, and reservoir deformation.

• The study highlights that temperature differentials between injected fluids and the reservoir can significantly influence stress evolution and fracture pressure, a factor often overlooked in conventional SWD modeling.

3) Probabilistic Forecasting of Maximum Injection Volume

• Monte Carlo simulation, combined with Latin Hypercube Sampling (LHS), provided a probabilistic assessment of maximum sustainable injection capacity, accounting for uncertainties in geomechanical and reservoir properties.

• The results demonstrate that formation integrity can be preserved by ensuring injection pressures remain below the estimated fracture gradient, reducing risks of fault reactivation and induced seismicity.

4) Practical Implications for SWD Well Design and Surveillance

• The developed methodology enables efficient injection surveillance by identifying pressure sensitive regions, optimizing well placement, and ensuring long-term disposal feasibility.

• The analytical model offers a computationally efficient alternative to full numerical simulations, making it suitable for regulatory compliance evaluations, operational decision-making, and reservoir management strategies.

References

Aamri, Mohammed, Al Zadjali, Ruqaya, Mahajan, Sandeep et al. 2017. Geomechanical Assessment of Injection Pressure Constraints for a Waterflood Field Development. *Proc., SPE Reservoir Characterisation and Simulation Conference and Exhibition*.

Ali, Sherif M., Le Bras, Ronan J., Medinskaya, Tatiana et al. 2022. Earthquake catalog improvements and their seismic hazard impacts for the Arabian Peninsula. *Journal of King Saud University - Science* **34** (4): 101934.

Anderson, Ernest Masson. 1951. *The dynamics of faulting and dyke formation with applications to Britain*.

Arno, Z., & Ove, S. 2010. *Stress Field of the Earth's Crust.*: Springer.

Bennion, D.B., Bennion, D.W., Thomas, F.B. et al. 1998. Injection Water Quality-A Key Factor to Successful Waterflooding. *Journal of Canadian Petroleum Technology* **37** (06).

Biot, M. A. and Willis, D. G. 2021. The Elastic Coefficients of the Theory of Consolidation. *Journal of Applied Mechanics* **24** (4): 594-601.

Chang, K. W. and Segall, P. 2016. Injection-induced seismicity on basement faults including poroelastic stressing. *Journal of Geophysical Research: Solid Earth **121*** (*4*): 2708-2726.

Clark, CE and Veil, JA. 2009. Produced water volumes and management practices in the United States. Pittsburgh, Pennsylvania, 23-25 February. https://onepetro.org/SPEGTS/proceedings-abstract/10UGC/All-10UGC/SPE-131784-MS/107737.

Clement Okezie, Chinemerem and Bump, Alex. 2024. Calibrating Performance Predictions for Large-Scale Injection. *Alexander and hovorka, susan, Calibrating Performance Predictions for Large-Scale Injection (December 20, 2024)*.

Eaton, Ben A. 1969. Fracture Gradient Prediction and Its Application in Oilfield Operations. *Journal of Petroleum Technology* **21** (10): 1353-1360.

Ganat, Tarek, Hrairi, Meftah, Badawy, Amr et al. 2024. Advancing sandstone reservoir compressibility prediction: A correlation-driven methodology. *Petroleum Research*.

Ganjdanesh, Reza and Hosseini, Seyyed A. 2018. Development of an analytical simulation tool for storage capacity estimation of saline aquifers. *International Journal of Greenhouse Gas Control* **74**: 142-154.

Hamid, Osman, Omair, Ahmed, and Guizada, Pablo. 2017. Reservoir Geomechanics in Carbonates. *Proc.,* In *Proc. SPE Middle East Oil & Gas Show and Conference*. https://doi.org/10.2118/183704-MS.

Hassan, Anas M., Mohyaldinn, Mysara Eissa, Ayoub, Mohammed A. et al. 2023. Chapter 7 - Interactions during various enhanced oil recovery operations. In *Developments in Petroleum Science*, ed. Ibnelwaleed A. Hussein and Mohamed Mahmoud, Vol. 78, 181-246. Elsevier.

Hosseini, Seyyed A., Kim, Seunghee, and Zeidouni, Mehdi. 2014. DKJStartApplication of multi-well analytical models to maximize geological CO2 storage in brine formations. *Energy Procedia* **63**: 3563-3567.

Hubbert, M King and Willis, David G. 1957. Mechanics of hydraulic fracturing. *Transactions of the AIME* **210** (01): 153-168.

Iman, Ronald L. 2008. Latin hypercube sampling. In *John Wiley & Sons, Ltd*.

Jing, Zhiyi and Wu, Xingru. 2019. Stochastic Determination of Formation Parting Pressure and Dynamic Injectivity for Water Injection. *Proc.,* 53rd US Rock Mechanics/Geomechanics Symposium.

Kang, H. 2010. In-situ stress measurements and stress distribution characteristics in underground.

Khan, Jawad Ali and Michael, Andreas. 2024. Wellbore Integrity Challenges in Saltwater Disposal: Case Study on the Fort Worth Basin. *Proc.,* SPE International Conference and Exhibition on Formation Damage ControlD011S002R006.

Kim, Yeseul, Lee, Changyeol, and Lee, Eun Young. 2018. Numerical analysis of sedimentary compaction: Implications for porosity and layer thickness variation: Implications for porosity and layer thickness variation. *지질학회지* **54** (6): 631-640.

Li, Cong, Ding, Lifen, An, Runze et al. 2024. Design of water nozzle shape and structure optimization for eccentric injection mandrel in water injection wells. *Journal of Petroleum Exploration and Production Technology* **14** (5): 1189-1204.

Li, Peng, Guo, QF, Liu, HT et al. 2017. Characteristics of current in-situ stress field and stress accumulation in Shandong region. *Chinese Journal of Rock Mechanics and Engineering* **36** (9): 2220-2231.

Lu, Yu, Li, Haitao, Lu, Cong et al. 2019. Predicting the fracture initiation pressure for perforated water injection wells in fossil energy development. *International Journal of Hydrogen Energy **44*** (31): 16257-16270.

M.R.P. Tingaya, *, R.R. Hillisa. 2002. Variation in vertical stress in the Baram Basin, Brunei:. *2004 Elsevier Ltd*.

Ma, Y. Z., Sobernheim, David, Garzon, Janz R. . 2016. Chapter 19 - Glossary for Unconventional Oil and Gas Resource Evaluation and Development. In *Unconventional Oil and Gas Resources Handbook*, ed. Y. Zee Ma and A. Holditch Stephen, 513-526. Boston: Gulf Professional Publishing.

Marbun, Bonar Tua Halomoan. 2015. A new approaching method to estimate fracture gradient by correcting Matthew–Kelly and Eaton's stress ratio. *Journal of Petroleum Science and Engineering* **135**: 261-267.

Matthews, WR. 1967. How to predict formation pressure and fracture gradient from electric and sonic logs. *Oil and Gas* **20**: 92-106.

Morgenstern, N. 1962. A relation between hydraulic fracture pressures and tectonic stresses. *Geofisica pura e applicata* **52** (1): 104-114.

Murray, Kyle E. 2014. Class II underground injection control well data for 2010–2013 by geologic zones of completion, Oklahoma. *Oklahoma Geological Survey Open File Report OF1* **32**.

Ousterhout, Ray S. and Hall, Colby D. 1961. Reduction of Friction Loss in Fracturing Operations. *Journal of Petroleum Technology* **13** (03): 217-222.

Perkins, T. K. and Gonzalez, J. A. 1985. The Effect of Thermoelastic Stresses on Injection Well Fracturing. *Society of Petroleum Engineers Journal **25*** (1): 78-88.

Ramey, HJ. 1970. Approximate solutions for unsteady liquidflow in composite reservoirs. *SPE-114173-PA* **9** (01).

Salemi, Hossein, Yurikov, Alexy, Lebedev, Maxim et al. 2021. A novel approach to determine the Biot's coefficient using X-ray computed tomography. *Bulletin of Engineering Geology and the Environment* **80** (10): 7865-7877.

Saripalli, K. P., Sharma, M. M., and Bryant, S. L. 2000. Modeling injection well performance during deep-well injection of liquid wastes. *Journal of Hydrology* **227** (1): 41-55.

Scanlon, Bridget R, Reedy, Robert C, Xu, Pei et al. 2020. Can we beneficially reuse produced water from oil and gas extraction in the US? *Science of The Total Environment* **717**: 137085. https://www.sciencedirect.com/science/article/pii/S0048969720305957?via%3Dihub.

Schmidt, Darren D, Bader, Jeffrey W, Day, Ashleigh et al. 2021. Completion Design Evolution for Saltwater Disposal Injection Wells in the Bakken Play. *Proc.,* SPE/AAPG/SEG Unconventional Resources Technology ConferenceD031S075R003.

Segall, P. and Lu, S. 2015. Injection-induced seismicity: Poroelastic and earthquake nucleation effects. *Journal of Geophysical Research: Solid Earth* ***120*** (7): 5082-5103.

Sharma, Mukul M., Pang, Shutong, Wennberg, Kjell Erik et al. 1997. Injectivity Decline in Water Injection Wells: An Offshore Gulf of Mexico Case Study. *Proc.,* SPE European Formation Damage Conference.

Shields, Michael D and Zhang, Jiaxin. 2016. The generalization of Latin hypercube sampling. *Reliability Engineering & System Safety* **148**: 96-108.

Stoian, E. 1965. Fundamentals and Applications of the Monte Carlo Method. *Journal of Canadian Petroleum Technology* **4** (03): 120-129. https://doi.org/10.2118/65-03-02.

Sun, Fengrui, Yao, Yuedong, Li, Xiangfang et al. 2018. Effect of friction work on key parameters of steam at different state in toe-point injection horizontal wellbores. *Journal of Petroleum Science and Engineering* **164**: 655-662.

Tabatabaee Moradi, Seyyed Shahab and Nikolaev, Nikolay Ivanovich. 2020. Uncertainty assessment of wellbore stability analysis in horizontal sections. *SN Applied Sciences* **2** (3): 437. https://doi.org/10.1007/s42452-020-2237-y.

Wu, Xingru, Childers, David R, Dai, Lei et al. 2023. Determining the Storage Capacity of a Saltwater Disposal Reservoir in Practice. *Proc.,* SPE Western Regional MeetingD031S011R001.

Wu, Zhiyi Jing;Xingru. 2017. Stochastic determination of formation parting pressure and dynamic injectivity for water injection. *Paper presented at the 53rd US Rock Mechanics/Geomechanics Symposium New York, NY, USA*.

Zhang, Jincai, Fan, Xin, Huang, Zhiwen et al. 2023. In situ stress determination in isotropic and anisotropic rocks and its application to a naturally fractured reservoir. *Geomechanics and Geophysics for Geo-Energy and Geo-Resources* **9** (1): 51.

Zhang, Jincai and Yin, Shang-Xian. 2017. Fracture gradient prediction: an overview and an improved method. *Petroleum Science* **14** (4): 720-730.

Zoback, Mark D. 2002. 34 State of stress in the Earth's lithosphere. *International Geophysics series* **81**: 559, XI-568, XII.

APPENDIX: PRESSURE SUPERPOSITION IN THE PROJECT AREA

The superposition technique determines the distribution of pressure buildup for a multiwell injection/extraction scenario. Defining the dimensionless terms using Darcy units as follows:

Dimensionless time:

$$t_D = \frac{2\pi kt}{\phi\mu c_t r_w^2} \qquad (A-1)$$

Dimensionless pressure:

$$p_D = \frac{2\pi kh}{q\mu B}\left[p_i - p\right] \qquad (A-2)$$

Dimensionless distance:

$$r_D = \frac{r}{r_w} \qquad (A-3)$$

In these definitions, the parameters are as follows:
tD – dimensionless time
k – permeability
t – time
φ – porosity
μ - fluid viscosity
ct – total compressibility
pD – dimensionless pressure
B- formation volume factor
pi – initial pressure
rD – dimensionless radius
r – radial distance
rw – wellbore radius

Case 1 – Infinite Acting Boundary Condition

For an infinite-boundary condition with several injectors, the normalized bottom hole pressure of a reference well 1, P_{WD}, is:

$$P_{WD_1} = \left\{ \begin{array}{l} \left[\frac{1}{2}\left(\ln\left(t_D\right) + 0.80908\right)\right] \\ + \sum_{i=1}^{Nw-1} q_{Di}\left[-\frac{1}{2}E_i\left(\frac{-r^2_{1-2}}{4t_D}\right)\right] \end{array} \right\} \qquad (A-4)$$

For the infinite-boundary condition with number of extractors, N_{wExt} , normalized bottomhole pressure of a reference well, P_{WDExt} , is:

$$P_{WDExt} = \left\{ \begin{array}{l} \left[\frac{1}{2} \left(\ln \left(t_{Dext} \right) + 0.80908 \right) \right] \\ + \sum_{i=1}^{N_{wExt}-1} q_{DExti} \left[-\frac{1}{2} Ei \left(\frac{-r^2_{DExti}}{4t_{Dext}} \right) \right] \end{array} \right\} \qquad (A-5)$$

In the following derivation and equations, we use Nw as the total number of wells, r_{i-j} represents the dimensionless distance from point i to point j.

qDi is the relative injection rate concerning the well,

rDi is the normalized radius,

Ei is the exponential integral function.

The pressure at any location in the reservoir is computed by summing the individual pressure contribution from each well. For a three-well injection system, the total pressure change is.

$\Delta P = \Delta P_1 + \Delta P_2 + \Delta P_3$

Each well contributes to the pressure buildup and their combined effect must be accounted for the matrix representation for muti-well pressure superposition.

The same technique can be applied to analyze the pressure distribution for a combination of pressure buildup and drawdown for a multi-well injection and extraction scenario. While calculating bottom hole pressure, given constant injection and extraction rates, is straightforward, determining constant injection and extraction rates for a given pressure limit in a reversed way requires some computational effort. For a two-well injection system with one extractor in an infinite-boundary reservoir, the combination of equations above can be rearranged into a matrix form, where matrix A and vectors B and Q can be written as follows:

[A][Q] = [B]

Where the relationship between the pressure and the flow rates is expressed as follows:

$$\bar{A} = \left[\begin{array}{ccc} \left[\frac{1}{2} \left(\ln \left(t_D \right) + 0.80908 \right) \right] & \left[-\frac{1}{2} E_i \left(\frac{-r^2_{D\,1-2}}{4t_D} \right) \right] & \left[-\frac{1}{2} Ei \left(\frac{-r^2_{Dext\,1-3}}{4t_{Dext}} \right) \right] \\ \left[\frac{-1}{2} E_i \left(\frac{-r^2_{D\,2-1}}{4t_D} \right) \right] & \left[\frac{1}{2} \left(\ln \left(t_D \right) + 0.80908 \right) \right] & \left[-\frac{1}{2} Ei \left(\frac{-r^2_{Dext\,2-3}}{4t_{Dext}} \right) \right] \\ \left[\frac{-1}{2} E_i \left(\frac{-r^2_{D\,3-1}}{4t_D} \right) \right] & \left[\frac{-1}{2} E_i \left(\frac{-r^2_{D\,3-2}}{4t_D} \right) \right] & \left[\frac{1}{2} \left(\ln \left(t_D \right) + 0.80908 \right) \right] \end{array} \right] \qquad (A-6)$$

$$\bar{B} = \begin{bmatrix} \dfrac{2\pi hkK\overline{rw}\left(P_{max} - P_1\right)}{\mu_w} \\ \dfrac{2\pi hkK\overline{rw}\left(P_{max}' - P_2\right)}{\mu_w} \\ \dfrac{2\pi hkK\overline{rw}\left(P_{max}' - P_3\right)}{\mu_w} \end{bmatrix} \qquad (A-7)$$

$$\bar{Q} = \begin{bmatrix} q_1 \\ q_2 \\ q_3 \end{bmatrix} \qquad (A-8)$$

where

Pmax and Pmin are the maximum allowable pressure of injectors and the minimum allowable bottomhole pressure of extractors, respectively. P1, P2, P3 refer to the pressure in wells 1, 2 and 3 respectively. The most important parameter that affects the formation integrity must be the maximum formation pressure in the above equation.

Case 2- Closed Boundary Condition

Similarly, for closed boundary conditions, with several injectors, the normalized bottom hole pressure of a well, P_{WD} , is:

$$P_{WD} = \left\{ \left[\left(P^s_{wd} \right) \right] + \left[\sum_{i=1}^{Nw-1} q_{Di} \left[\begin{array}{l} \dfrac{-1}{2} E_i \left(\dfrac{-r^2_{Di}}{4t_D} \right) + \dfrac{1}{2} E_i \left(\dfrac{-r^2_{eD}}{4t_D} \right) \\ + 2\dfrac{t_D}{r^2_{eD}} exp\left(\dfrac{-r^2_{eD}}{4t_D} \right) \end{array} \right] \right] \right\} \qquad (A-9)$$

P^S_{WD} refers to the late-time solution for the bottomhole pressure.

For a closed system the PSWD is:

$$P^S_{WD} = \left\{ \begin{array}{l} \left[\dfrac{1}{2} \left(\ln\left(t_D \right) + 0.80908 \right) \right] \\ + \left[\dfrac{1}{2} Ei\left(-\dfrac{r^2_{eD}}{4t_D} \right) + 2\dfrac{t_D}{r^2_{eD}} exp\left(-\dfrac{r^2_{eD}}{4t_D} \right) \right] \end{array} \right\} \qquad (A-10)$$

$$Let\ \Delta = \frac{1}{2} Ei\left(-\frac{r^2_{eD}}{4t_D} \right) + 2\frac{t_D}{r^2_{eD}} exp\left(-\frac{r^2_{eD}}{4t_D} \right)$$

where,

reD denotes the formation external boundary radius divided by the radius re/rw.

The system of equation above for the pressure distribution is represented in matrix form, which is used for solving multiple interacting wells efficiently.

$$\bar{A} = \begin{bmatrix} \left[P^S{}_{wD}\right] & \left[-\frac{1}{2}E_i\left(-\frac{r^2{}_{D\,1-2}}{4t_D}\right)+\Delta\right] & \left[-\frac{1}{2}E_i\left(-\frac{r^2{}_{D\,1-3}}{4t_D}\right)+\Delta\right] \\ -\left[\frac{1}{2}E_i\left(-\frac{r^2{}_{D\,2-1}}{4t_D}\right)+\Delta\right] & \left[P^S{}_{wD}\right] & \left[-\frac{1}{2}E_i\left(-\frac{r^2{}_{D\,2-3}}{4t_D}\right)+\Delta\right] \\ -\left[\frac{1}{2}E_i\left(-\frac{r^2{}_{D\,3-1}}{4t_D}\right)+\Delta\right] & \left[-\frac{1}{2}E_i\left(-\frac{r^2{}_{D\,3-2}}{4t_D}\right)+\Delta\right] & \left[P^S{}_{wD}\right] \end{bmatrix} \quad (A-11)$$

The matrix will be as follows, B and C will remain the same.

Case 3- Open Boundary conditions

In the case of open boundary conditions, the normalized bottom hole pressure of a reference well 1, P_{WD}, is:

$$P_{WD} = P^s{}_{wd} + \sum_{i=1}^{Nw-1} q_{Di}\left[\frac{-1}{2}E_i\left(\frac{-r^2{}_{Di}}{4t_D}\right) + \frac{1}{2}E_i\left(\frac{-r^2{}_{eD}}{4t_D}\right)\right] \quad (A-12)$$

For an open boundary system, the $P^S{}_{WD}$ is:

$$P^S{}_{wD} = \frac{1}{2}\left(\ln\left(t_D\right)+0.80908\right) + \frac{1}{2}Ei\left(-\frac{r^2{}_{eD}}{4t_D}\right) \quad (A-13)$$

$$Let\ \Delta = \frac{1}{2}E_i\left(\frac{-r^2{}_{eD}}{4t_d}\right)\ in\ this\ case$$

By combining equations, for open case boundary the following matrix can be calculated -

$$\bar{A} = \begin{bmatrix} P^S{}_{wD} & -\frac{1}{2}E_i\left(-\frac{r^2{}_{D,1-2}}{4t_D}\right)+\Delta & -\frac{1}{2}E_i\left(-\frac{r^2{}_{D,1-3}}{4t_D}\right)+\Delta \\ -\frac{1}{2}E_i\left(-\frac{r^2{}_{D,2-1}}{4t_D}\right)+\Delta & P^S{}_{wD} & -\frac{1}{2}E_i\left(-\frac{r^2{}_{D,2-3}}{4t_D}\right)+\Delta \\ -\frac{1}{2}E_i\left(-\frac{r^2{}_{D,3-1}}{4t_D}\right)+\Delta & -\frac{1}{2}E_i\left(-\frac{r^2{}_{D,3-2}}{4t_D}\right)+\Delta & P^S{}_{wD} \end{bmatrix} \quad (A-14)$$

The appendix provides an analytical framework for modeling multi-well pressure interactions. We can estimate the reservoir pressure distribution over time using the following matrix. This matrix also helps us to compute the maximum allowable injection volume, ensuring the formation integrity while minimizing seismic risk.